

1854

USGS-OFR-85-49

USGS-OFR-85-49

UNITED STATES  
DEPARTMENT OF THE INTERIOR  
GEOLOGICAL SURVEY

PRELIMINARY INTERPRETATION OF PALEOMAGNETIC AND MAGNETIC  
PROPERTY DATA FROM DRILL HOLES USW G-1, G-2, GU-3, G-3,  
AND VH-1 AND SURFACE LOCALITIES IN THE VICINITY OF  
YUCCA MOUNTAIN, NYE COUNTY, NEVADA

By

J. G. Rosenbaum and D. B. Snyder

UNITED STATES  
DEPARTMENT OF THE INTERIOR  
GEOLOGICAL SURVEY

PRELIMINARY INTERPRETATION OF PALEOMAGNETIC AND MAGNETIC  
PROPERTY DATA FROM DRILL HOLES USW G-1, G-2, GU-3, G-3,  
AND VH-1 AND SURFACE LOCALITIES IN THE VICINITY OF  
YUCCA MOUNTAIN, NYE COUNTY, NEVADA

By

J. G. Rosenbaum and D. B. Snyder

## CONTENTS

	Page
Abstract.....	1
Introduction.....	2
Sampling Procedure.....	2
Laboratory Procedure.....	3
Results.....	4
Paintbrush Tuff.....	4
Tiva Canyon Member.....	4
Yucca Mountain and Pah Canyon Members.....	11
Topopah Spring Member.....	17
Tuffaceous beds of Calico Hills.....	29
Crater Flat Tuff.....	33
Prow Pass Member.....	33
Bullfrog Member.....	39
Tram Member.....	45
Other units.....	50
Lava flows and flow breccias between the Tram Member and the Lithic Ridge Tuff.....	50
Lithic Ridge Tuff.....	54
Older tuffs of USW G-1 and lava flows and flow breccias of USW G-2.....	54
Discussion and Summary.....	65
References.....	72

## ILLUSTRATIONS

Figure 1.	Location of drill holes and outcrop sampling sites in the vicinity of Yucca Mountain.....	5
2.	Equal area projection of paleomagnetic data for the Tiva Canyon Member of the Paintbrush Tuff.....	7
3.	Paleomagnetic data versus depth for the Yucca Mountain, Pah Canyon and Tiva Canyon Members of the Paintbrush Tuff.....	8
4.	Intensity of natural remanent magnetization and susceptibility versus depth for the Yucca Mountain, Pah Canyon and Tiva Canyon Members of the Paintbrush Tuff.....	10
5.	Equal area projection of paleomagnetic data for the Yucca Mountain and Pah Canyon Members of the Paintbrush Tuff.....	14
6.	Equal area projection of paleomagnetic data for the Topopah Spring Member of the Paintbrush Tuff.....	19
7.	Paleomagnetic data versus depth for the Topopah Spring Member of the Paintbrush Tuff.....	24
8.	Intensity of natural remanent magnetization and susceptibility versus depth for the Topopah Spring Member of the Paintbrush Tuff.....	28
9.	Paleomagnetic inclinations versus depth for the tuffaceous beds of Calico Hills.....	30

ILLUSTRATIONS--CONTINUED

	Page
Figure 10. Intensity of natural remanent magnetization and susceptibility versus depth for the for the tuffaceous beds of Calico Hills.....	32
11. Equal area projection of paleomagnetic data for the Prow Pass Member of the Crater Flat Tuff.....	35
12. Paleomagnetic inclinations versus depth for the Prow Pass Member of the Crater Flat Tuff.....	36
13. Intensity of natural remanent magnetization and susceptibility versus depth for the Prow Pass Member of the Crater Flat Tuff.....	38
14. Equal area projection of paleomagnetic data for the Bullfrog and Tram Members of the Crater Flat Tuff.....	41
15. Paleomagnetic inclinations versus depth for the Bullfrog Member of the Crater Flat Tuff.....	42
16. Intensity of natural remanent magnetization and susceptibility versus depth for the Bullfrog Member of the Crater Flat Tuff.....	44
17. Paleomagnetic inclinations versus depth for the Tram Member of the Crater Flat Tuff.....	47
18. Intensity of natural remanent magnetization and susceptibility versus depth for the Tram Member of the Crater Flat Tuff.....	49
19. Paleomagnetic inclinations versus depth for the dacite and rhyodacite lava flows and flow breccias between the Tram Member of the Crater Flat Tuff and the Lithic Ridge Tuff.....	51
20. Intensity of natural remanent magnetization and susceptibility versus depth for the dacite and rhyodacite lava flows and flow breccias between the Tram Member of the Crater Flat Tuff and the Lithic Ridge Tuff.....	53
21. Paleomagnetic inclinations versus depth for the Lithic Ridge Tuff.....	56
22. Equal area projection of paleomagnetic data for the Lithic Ridge Tuff.....	57
23. Intensity of natural remanent magnetization and susceptibility versus depth for the Lithic Ridge Tuff..	64
24. Intensity of total magnetization versus depth for drill holes USW G-1, G-2, GU-3 and G-3, and a modeled total field log for drill hole USW G-1.....	68

TABLES

	Page
Table 1. Paleomagnetic directional data for the Tiva Canyon Member of the Paintbrush Tuff, the Tuff of Chocolate Mountain, and the Tuff of Pinion Pass.....	6
2. Magnetic property data for the Tiva Canyon Member of the Paintbrush Tuff and the Tuff of Chocolate Mountain.....	9

TABLES--CONTINUED

Table		Page
3.	Paleomagnetic directional data for the Yucca Mountain Member of the Paintbrush Tuff.....	12
4.	Paleomagnetic directional data for the Pah Canyon Member of the Paintbrush Tuff.....	13
5.	Magnetic property data for the Yucca Mountain Member of the Paintbrush Tuff.....	15
6.	Magnetic property data for the Pah Canyon Member of the Paintbrush Tuff.....	16
7.	Paleomagnetic directional data for the Topopah Spring Member of the Paintbrush Tuff.....	18
8.	Magnetic property data for the Topopah Spring Member of the Paintbrush Tuff.....	27
9.	Magnetic property data for the tuffaceous beds of Calico Hills.....	31
10.	Paleomagnetic directional data for the Prow Pass Member of the Crater Flat Tuff.....	34
11.	Magnetic property data for the Prow Pass Member of the Crater Flat Tuff.....	37
12.	Paleomagnetic directional data for the Bullfrog Member of the Crater Flat Tuff.....	40
13.	Magnetic property data for the Bullfrog Member of the Crater Flat Tuff.....	43
14.	Paleomagnetic directional data for the Tram Member of the Crater Flat Tuff.....	46
15.	Magnetic property data for the Tram Member of the Crater Flat Tuff.....	48
16.	Magnetic property data for the dacite and rhyodacite lava flows and flow breccias between the Tram Member of the Crater Flat Tuff and the Lithic Ridge Tuff.....	52
17.	Paleomagnetic directional data for the Lithic Ridge Tuff.....	55
18.	Magnetic property data for the Lithic Ridge Tuff.....	63
19.	Paleomagnetic directional data for the older tuffs of USW G-1.....	66
20.	Magnetic property data for rocks older than the Lithic Ridge Tuff.....	67
21.	Paleomagnetic polarities of volcanic rocks at Yucca Mountain.....	70

UNITED STATES  
DEPARTMENT OF THE INTERIOR  
U.S. GEOLOGICAL SURVEY

PRELIMINARY INTERPRETATION OF PALEOMAGNETIC AND MAGNETIC  
PROPERTY DATA FROM DRILL HOLES USW G-1, G-2, GU-3, G-3,  
AND VH-1 AND SURFACE LOCALITIES IN THE VICINITY OF  
YUCCA MOUNTAIN, NYE COUNTY, NEVADA

By

J. G. Rosenbaum and D. B. Snyder

ABSTRACT

Measurements of magnetic properties and paleomagnetic directions have been made on thousands of samples of Miocene age volcanics from drill core and surface localities in and around Yucca Mountain at the Nevada Test Site. The directional data have firmly established paleomagnetic polarities for the various members of the Paintbrush and Crater Flat Tuffs, and for the Tuffaceous Beds of Calico Hills. In addition, the Lithic Ridge Tuff is found to have a highly unusual paleomagnetic direction (southwest and nearly horizontal). Changes in inclination of remanence with depth in the Tuffaceous Beds of Calico Hills indicate that this unit was emplaced over a substantial period of time relative to secular variation of the geomagnetic field, and that the relatively thin sequence of tuffs of this unit encountered at the USW G-1 locality correlates roughly with the basal 125 m of the much thicker sequence penetrated in drill hole USW G-2.

Paleomagnetic data obtained for the Topopah Spring Member of the Paintbrush Tuff from cores from drill holes at Yucca Mountain and from outcrop at Busted Butte demonstrate that the remanence directions of this unit vary with depth. The cause of this variation is presently unknown and its presence severely limits the usefulness of the paleomagnetic method as a tool for examining structural rotations affecting the Topopah Spring Member. In contrast, the Tiva Canyon Member of the Paintbrush Tuff yields essentially one direction of remanence everywhere it has been sampled at Yucca Mountain. The near coincidence of paleomagnetic directions obtained for Tiva Canyon sites from throughout Yucca Mountain indicates that the change in strike of eutaxitic foliation and of the base of this unit in the vicinity of Drill Hole Wash cannot be due to structural rotation about a vertical axis, but does not rule out rotations of a few degrees about horizontal axes.

Four widespread units, the Tiva Canyon and Topopah Spring Members of the Paintbrush Tuff and the Bullfrog and Tram Members of the Crater Flat Tuff, are identified as potential sources of significant magnetic anomalies by measurements of remanent intensity and susceptibility. The measurements also demonstrate large variations in remanent intensity and susceptibility within individual ash-flow sheets. In some cases these variations are closely

related to geologically recognizable breaks in ash-flow tuff deposition. These variations provide the possibility of using magnetic field logs not only to locate major stratigraphic contacts but also to map subunits within the major ash-flow sheets.

## INTRODUCTION

The strata underlying Yucca Mountain comprise a thick sequence of Miocene age volcanic rocks. The Tiva canyon Member of the Paintbrush Tuff is exposed over most of the surface of Yucca Mountain. Nearly 2 kilometers of ash-flow tuffs and related bedded tuffs were penetrated in drill holes USW G-1, G-2, GU-3, and G-3. In descending stratigraphic order the units are the Tiva Canyon, Yucca Mountain, Pah Canyon, and Topopah Spring Members of the Paintbrush Tuff, the tuffaceous beds of Calico Hills, the Prow Pass, Bullfrog and Tram Members of the Crater Flat Tuff, unnamed rhyodacite and dacite lava flows and flow breccias, the Lithic Ridge Tuff, and unnamed older lavas and tuffs. Detailed lithologic descriptions of the drill core are provided by Spengler and others [1981], Maldonado and Koether [1983], and Scott and Castellanos [1984].

Measurements of remanent magnetization and magnetic susceptibility of samples of volcanic rocks from bore holes and surface outcrops in the vicinity of Yucca Mountain have been used as stratigraphic correlation tools, as limitations on structural interpretations [Spengler and Rosenbaum, 1980], and as guides to the interpretation of magnetic anomalies in the area [Bath and Jahren, 1984]. Also these data should prove useful in the interpretation of in-hole magnetic-field and magnetic-susceptibility logs.

While the direction of remanent magnetism is useful in volcanic stratigraphic correlation and in the solution of structural problems, the direction and intensity of total magnetization,  $\vec{J}_t$ , is needed for the interpretation of magnetic anomalies. The total magnetization of a rock specimen is the vector sum of its remanent and induced magnetizations, so that

$$\vec{J}_t = \vec{J}_r + \vec{J}_i = \vec{J}_r + \frac{K}{\mu_0} \vec{B}$$

where  $\vec{J}_t$ ,  $\vec{J}_r$ , and  $\vec{J}_i$  are total, remanent, and induced magnetizations in amperes per meter ( $\text{Am}^{-1}$ ), respectively;  $K$  is the bulk susceptibility (dimensionless);  $B$  is the magnetic flux ( $\vec{B}$  has a magnitude of about  $0.517 \times 10^{-4}$  tesla (T) at NTS); and  $\mu_0$  is the permeability of free space ( $\mu_0 = 4\pi \times 10^{-7} \text{TmA}^{-1}$ ).  $\vec{J}_r$  and  $K$  can be easily measured in the laboratory.

The purpose of this report is to document magnetic property data for specimens collected during 1980-83 from drill holes USW G-1, G-2, GU-3, G-3, and VH-1 as well as from surface sampling localities on and around Yucca Mountain. Preliminary interpretations are also presented.

## SAMPLING PROCEDURE

Cylindrical samples, approximately 2.5 cm in both length and diameter, were collected from outcrops and drill core. A sun compass was used to orient outcrop samples [Creer and Sanver, 1967]. Orientation with respect to the drill hole axes was maintained for all samples collected from drill core. In addition, samples from oriented core segments were collected in a

manner which preserved the orientation information [Spengler and Rosenbaum, 1980].

Sampling of outcrops has the advantage that accurate orientation of all samples is easily obtained by standard techniques. However, outcrop sampling has a number of disadvantages: (1) sampling is restricted to the limited stratigraphic section exposed in the area; (2) sampling vertically through a unit is often difficult due to incomplete exposure; (3) magnetic properties of samples may have been affected by weathering and therefore may not be representative of a large volume of rock; and (4) remanent magnetism at some localities has been altered by lightning strikes. Sampling cores from deep drill holes eliminates these problems. However, oriented core was obtained for only a small percentage of the drilled section because azimuthal orientation of deep drill cores is difficult and expensive. Also the magnitude of the errors involved in the orienting procedure are much greater than those for outcrop sampling. Thus, the declination of magnetic remanence cannot be obtained for most of the samples taken from the deep drill holes. Moreover, it should be noted that inclination values from unoriented core cannot be corrected for deviation of the drill hole from vertical. Therefore, directional data from oriented samples presented on equal-area projections and in tables have been corrected for the drill hole orientation, whereas the inclination data for all samples plotted versus depth is oriented with respect to the drill hole axis.

#### LABORATORY PROCEDURES

The natural remanent magnetism (NRM) of each specimen was measured with a spinner magnetometer or, in some cases, with a cryogenic magnetometer. All outcrop samples were subjected to progressive alternating field (af) demagnetization to isolate a stable remanence direction. Selected samples from each unit encountered in the drill cores were also subjected to progressive af demagnetization to peak fields of 80 or 100 mT. In most cases it was found that the direction of these samples changed little during the cleaning process. All subsurface samples were demagnetized at a peak field of 10 mT.

Susceptibilities were determined on a precisely calibrated [Rosenbaum and others, 1979], highly sensitive bridge [Cristie and Symons, 1969]. A value of 51,700 nT was used for the earth's field in calculating the induced magnetization.

For the purpose of calculating total magnetization, each sample from drill core was assigned a remanent declination. In most cases the declination was obtained by averaging directions from measurements made on oriented specimens from the same geologic unit. In a few instances a declination of 0° (180°) was assigned to units which appeared to be normal (reversed) based on inclination data alone. In the text which follows "polarities," "directions," and "intensities of magnetization" refer to remanent magnetization unless otherwise specified as referring to total magnetization.

## RESULTS

### Paintbrush Tuff

**Tiva Canyon Member:** The Tiva Canyon Member was sampled extensively in outcrop and in drill hole USW GU-3 (Figure 1). Outcrop sampling sites for the Tiva Canyon Member range from near the base of the unit to near its top. The Tiva Canyon was sampled throughout most of its thickness at site SJ82-1 and in drill hole USW GU-3. In addition, a small number of samples of the Chocolate Mountain Tuff (intracaldera equivalent to the uppermost part of the Tiva Canyon Member) and of the closely associated Tuff of Pinon Pass [Byers and others, 1976; Christiansen and others, 1976] were obtained.

All samples are of reversed polarity. The directions obtained from the Chocolate Mountain Tuff and the Tuff of Pinon Pass are essentially indistinguishable from those determined for the Tiva Canyon Member (Table 1). The directional data from the Tiva Canyon Member at Yucca Mountain are closely grouped (Figures 2 and 3, and Table 1) indicating that the Tiva Canyon Member possesses essentially one direction of remanent magnetization throughout its thickness everywhere at Yucca Mountain. The close agreement of the directions from the Yucca Mountain block indicates that there has been little, if any, relative rotational deformation within Yucca Mountain since the emplacement of the Tiva Canyon. Although changes in the strike of eutaxitic foliation and of the base of the Tiva Canyon (see figure 6 in Spengler and Rosenbaum, 1980) cannot be due to rotation about a vertical axis, these data do not exclude the possibility of small rotations about horizontal axes. Alternatively, the changes in strike may be depositional rather than tectonic in nature.

The Tiva Canyon Member sampled in USW GU-3 exhibits large changes in both the intensity of remanent magnetization and susceptibility with depth. The variation in remanent intensity defines a relatively simple pattern; the values decrease abruptly with increasing depth from about  $2 \text{ Am}^{-1}$  to less than  $0.3 \text{ Am}^{-1}$  and then increase gradually to a depth of about 75 m (Figure 4). Below this depth the values alternately increase and decrease, defining three increasingly large maxima. Susceptibilities display a more complex pattern of variation which shows little correlation to that of the intensity of magnetization. The sharp increase of intensity and susceptibility at the top of the sampled section corresponds to an increase in phenocryst and mafic mineral content, and the intensity maximum at a depth of about 105 m occurs within the basal vitrophyre [Scott and Castellanos, 1984]. Also the rapid fall in intensity at the base of the unit corresponds to the decrease in welding at the base of the ash-flow sheet. No other correlation between intensity and/or susceptibility changes and changes in the lithology described by Scott and Castellanos [1984] are obvious.

Similar variations of susceptibility and magnetization occur at site SJ82-1 (Figure 4). Average values of magnetization and susceptibility from surface localities within the Yucca Mountain block are in good agreement with the data from USW GU-3 (Table 2). The highest average magnetizations are from sites M79-25, M79-26 and JR81-8 which are all located in a densely welded, columnarly jointed zone near the base of the Tiva Canyon Member. As in the results from USW GU-3, these high intensity values are associated with relatively low values of susceptibility. Sampling locality JR81-2 is located

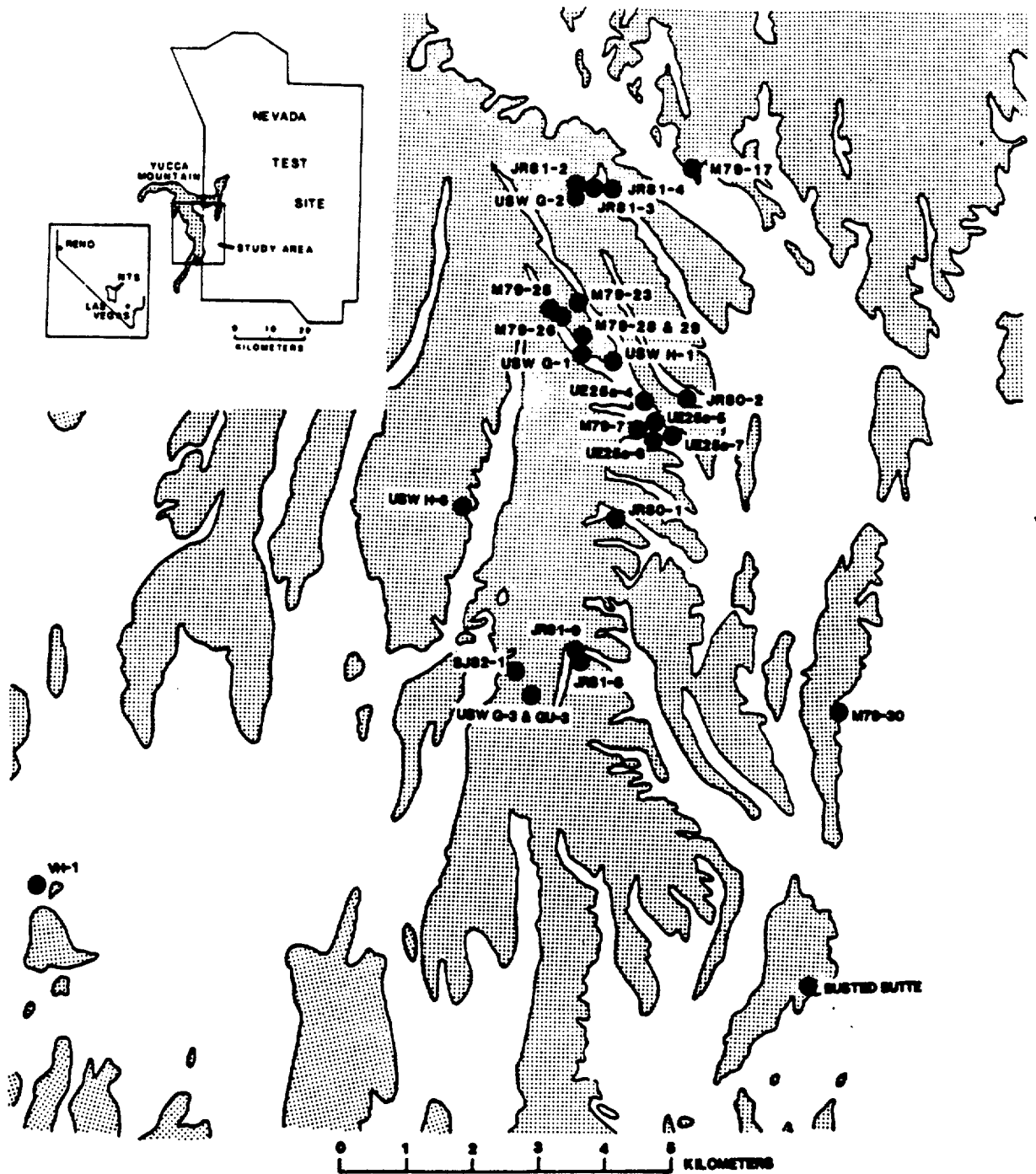


Figure 1.—Locations of drill holes and outcrop sampling sites in the vicinity of Yucca Mountain. Shading indicates area where bedrock is largely exposed.

Table 1. Directional data for the Tiva Canyon Member, the Chocolate Mountain Tuff, and the Tuff of Pinon Pass

Site	Lat.	Long.	N	$D_R$	$I_R$	$\alpha_{95}$	K	af	Comments
M79-7	36.851	116.447	5	168.8	-43.6	3.6	457.7	20-40	
M79-25	36.874	116.464	7	172.1	-40.6	3.6	281.3	20	
M79-26	36.871	116.463	5	164.7	-38.8	4.8	256.2	20	
M79-28	36.870	116.459	6	165.8	-40.9	3.5	359.0	20	
M79-29	36.870	116.459	8	165.0	-41.3	1.5	1393.9	20	
JR80-1	36.844	116.452	7	169.4	-44.9	2.8	461.3	20	
JR80-2	36.861	116.443	7	164.7	-40.5	1.6	1396.4	20	
JR81-2	36.892	116.461	9	167.9	-39.7	2.5	416.5	10	
JR81-8	36.824	116.459	6	175.7	-43.8	6.0	127.1	20	One sample may be from rotated block. Same data with rotated sample removed
			5	172.2	-42.8	2.3	1079.5	20	
SJ82-1	36.923	116.468	22	168.2	-42.3	3.9	64.9	20	
USW GU-3	36.816	116.467	11	177.5	-42.3	4.1	122.2	10	Depth 43.0-106.5 m. Depth 32.5-34.0 m. Core run apparently misoriented by 180°.
			5	345.2	-39.7	1.4	2795.9	10	
SJ82-9	36.930	116.468	3	166.0	-39.6	---	---	20	Tuff of Chocolate Mountain. Topopah Spring NW Quadrangle.
SJ82-5	36.945	116.472	3	164	-35	---	---	20	Tuff of Pinon Pass. Topopah Spring NW Quadrangle.
SJ82-6	36.938	116.458	2	160	-21	---	---	20	Tuff of Pinon Pass. Topopah Spring NW Quadrangle.
SJ82-9	36.930	116.468	3	165	-40	---	---	20	Tuff of Pinon Pass. Topopah Spring NW Quadrangle.

N is the number of samples used in calculating the mean.  $D_R$  and  $I_R$  are the average declination and inclination of remanence, respectively;  $\alpha_{95}$  is the half angle of the cone of 95% confidence; K is the Fisher precision parameter; af is the alternating field demagnetization step used to calculate the mean directions. --- indicates site not shown in Figure 1.

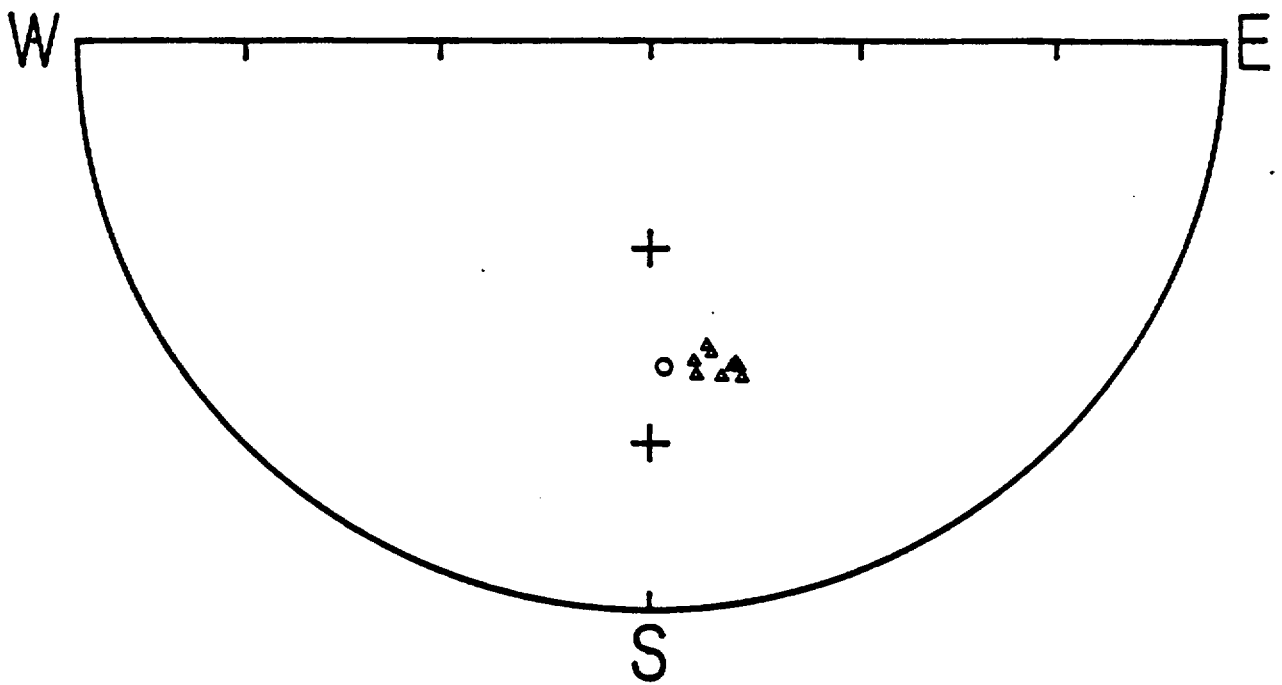


Figure 2.—Equal area projection of paleomagnetic data from the Tiva Canyon Member of the Paintbrush Tuff (Table 1). Triangles and circle are mean directions for outcrop sites and drill hole USW GU-3, respectively.

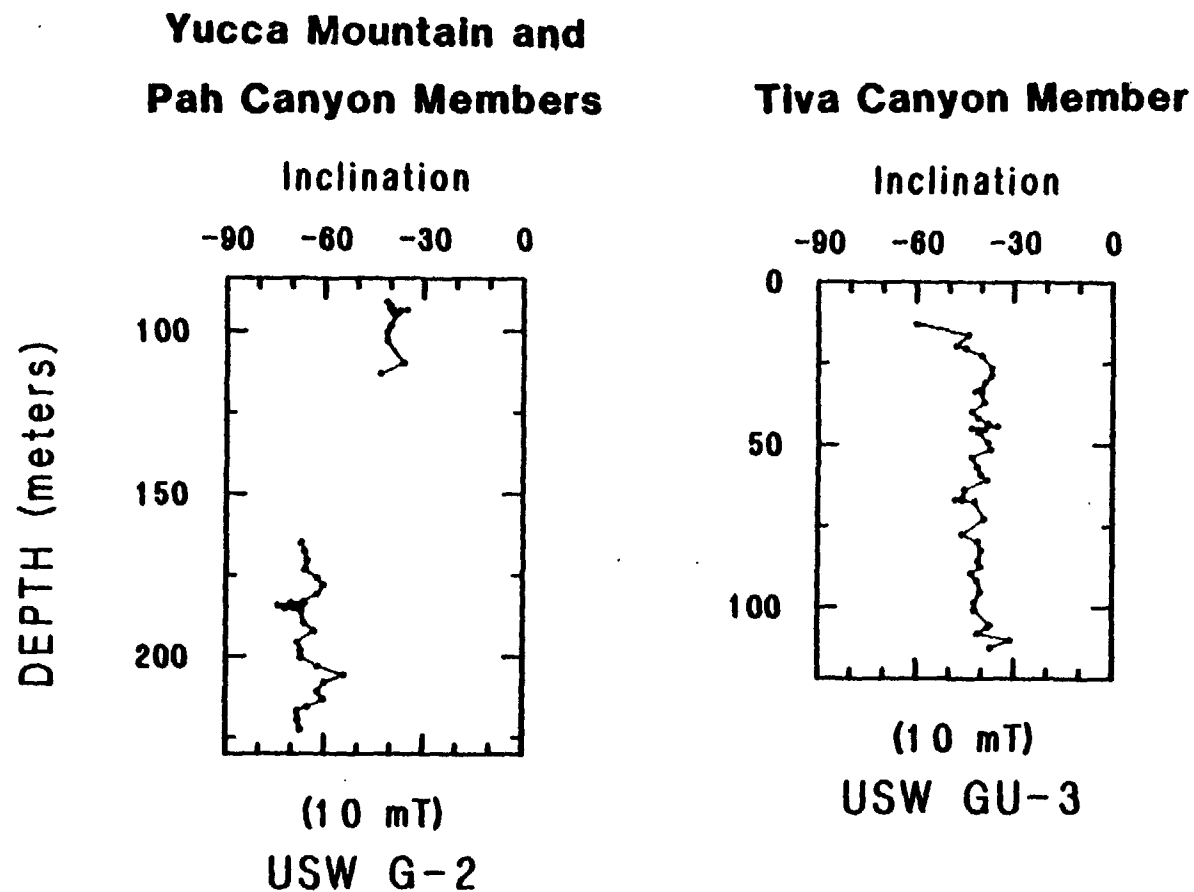


Figure 3.—Paleomagnetic data versus depth for the Yucca Mountain, Pah Canyon (from drill hole USW G-2) and Tiva Canyon (from drill hole USW GU-3 and site SJ82-1) Members of the Paintbrush Tuff after of demagnetization at the indicated fields. Elevations for site SJ82-1 are relative to the top of the Topopah Spring Member and were obtained by hand leveling.

Table 2. Magnetic Property data for the Tiva Canyon Member and the Chocolate Mountain Tuff

Site	N	$J_{NRM}$	Sus.	Q	$D_T$	$I_T$	$J_T$	Comments
M79-7	6 4	8.77±14.4 .523±.134	5.97±0.89 6.25±0.88	37.8 2.07	217 205	-46 -47	8.72±14.4 .445±.085	Two samples intensely magnetic (lightning?). Above 2 samples removed.
M79-25	7	3.89±2.90	2.06±1.08	40.2	170	-39	3.85±2.89	
M79-26	7(5)	4.80±3.45	2.97±1.16	36.3	170	-39	4.75±3.43	
M79-28	6	1.05±0.30	4.44±0.73	5.78	169	-39	.969±0.31	
M79-29	8	.553±.115	4.49±1.61	3.22	168	-35	.470±.088	
JR80-1	7	1.75±1.47	5.04±0.75	8.05	169	-42	1.66±1.46	
JR80-2	7	.392±.158	5.59±1.70	1.90	160	-26	.311±.160	
JR81-2	9	.570±.216	1.83±1.18	13.4	166	-36	.536±.232	
JR81-8	6	3.64±0.75	2.99±0.43	29.2	172	-42	3.58±0.75	
SJ82-1	13	1.15±1.22	3.92±3.62	9.5	162	-35	1.02±1.21	
USW GU-3	50	1.11±1.31	5.05±2.41	7.45	169	-23	.943±1.32	Assumed $D_R=175^\circ$ .
SJ82-9	3	10.1±8.18	11.33±5.47	20.3	165	-38	9.69±7.99	Chocolate Mountain Tuff.

N is the number of samples used in computing the means.  $J_{NRM}$  is the average intensity of natural remanent magnetization ( $A_m^{-1}$ ); Sus is SI susceptibility  $\times 10^3$ ; Q is the Königsberger ratio (ratio of  $J_{NRM}$  to induced magnetization); and  $D_T$ ,  $I_T$ , and  $J_T$  are the declination, inclination and intensity ( $A_m^{-1}$ ) of total magnetization, respectively.  $D_R$  is the declination of remanence assigned to the entire unit for the purpose of calculating total magnetization (see text).

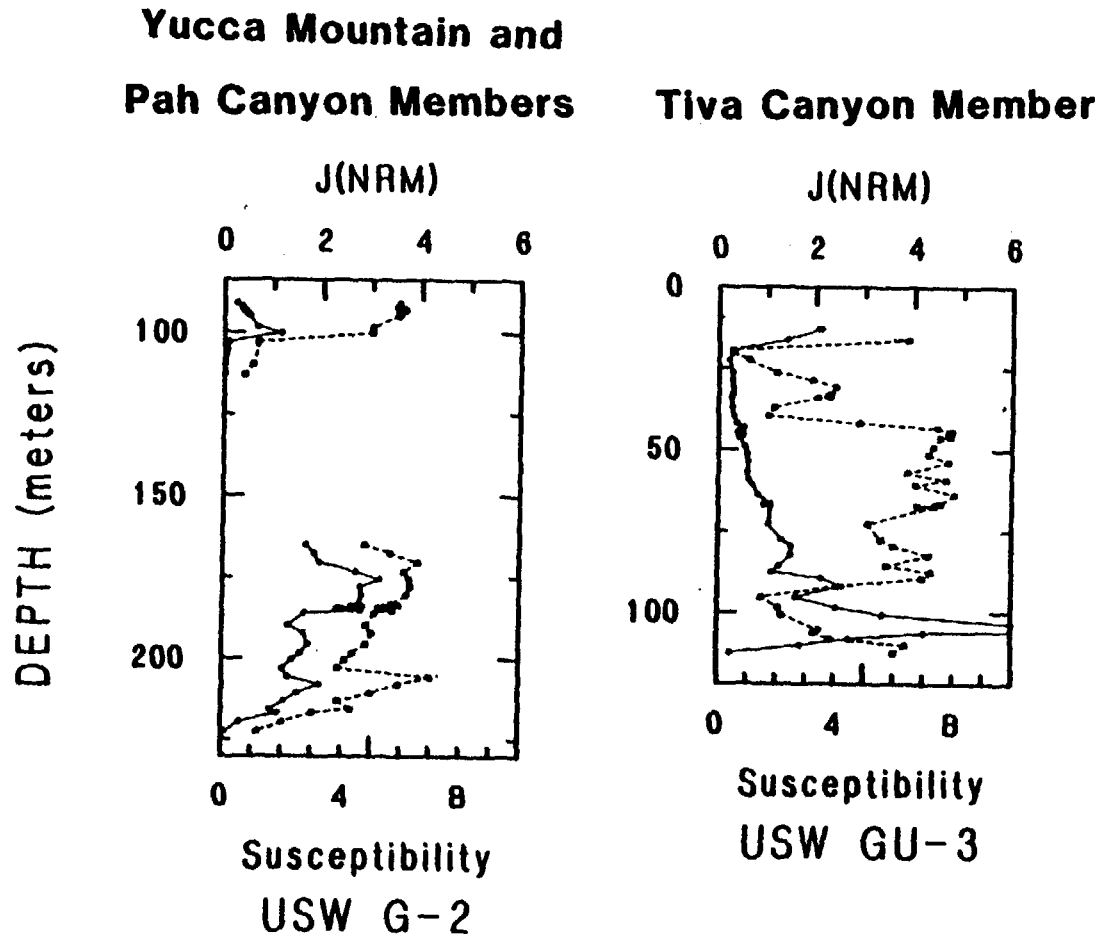


Figure 4.--Intensity of natural remanent magnetization,  $J(\text{NRM})$ , in  $\text{Am}^{-1}$  (circles and solid line) and SI susceptibility  $\times 10^3$  (squares and dashed line) for the Yucca Mountain, Pah Canyon (from drill hole USW G-2) and Tiva Canyon (from drill hole USW GU-3 and site SJ82-1) Members of the Paintbrush Tuff. Elevations for site SJ82-1 are as in Figure 3.

in the upper portion of the unit (below the cap rock) and is characterized by relatively low values of both susceptibility and magnetization. The other sites are located in the more central portion of the ash-flow tuff and possess relatively high susceptibilities and low to intermediate intensities. Three samples of the tuff of Chocolate Mountain from site SJ82-9 yield high values of both remanent intensity and susceptibility (Table 2).

**Yucca Mountain and Pah Canyon Members:** Two relatively thin local members of the Paintbrush Tuff, the Yucca Mountain and Pah Canyon Members, were each sampled at two outcrop localities (Figure 1). Oriented specimens of the Pah Canyon Member were also obtained from drill hole USW G-2. Both units are of reversed polarity with the inclination of remanence for the Pah Canyon Member being significantly steeper than that of the Yucca Mountain Member (Figures 3 and 5 and Tables 3 and 4).

Intensity and susceptibility data for the Yucca Mountain and Pah Canyon Members are presented in Figure 4 and Tables 5 and 6. The Yucca Mountain Member possesses low remanent intensities (average less than  $0.4 \text{ Am}^{-1}$ ) and relatively high susceptibilities so that values of  $Q$  for this unit are among the lowest determined in the area.

Susceptibilities of Pah Canyon Member samples are in the same general range as those of the Yucca Mountain Member. In contrast, the remanent intensities of the Pah Canyon Member average nearly an order of magnitude greater than those of the Yucca Mountain Member. Also, in contrast to the case for the Tiva Canyon Member, there is obviously a high degree of correlation between changes in remanent intensity and susceptibility in the Pah Canyon Member (Figure 4). It should be noted, however, that the maxima and minima for these curves are offset by a few meters.

Table 3. Directional data for the Yucca Mountain Member

Site	Lat.	Long.	N	D <sub>R</sub>	I <sub>R</sub>	a <sub>95</sub>	K	af	Comments
M79-23	36.876	116.460	7	184.9	-37.5	2.9	442.3	10	
JR81-3	36.892	116.458	8	179.1	-38.0	1.1	2612.9	20	

For explanation of headings see Table 1.

Table 4. Directional data for the Pah Canyon Member

Site	Lat.	Long.	N	D <sub>R</sub>	I <sub>R</sub>	a <sub>95</sub>	K	af	Comments
M79-17	36.892	116.440	6	149.1	-61.9	3.3	406.3	30	
JR81-4	36.892	116.455	7	157.7	-61.4	2.1	795.0	20	
USW G-2	38.890	116.459	7	140.6	-69.6	3.0	407.6	20	Depth 183.0-185.5 m.

For explanation of headings see Table 1.

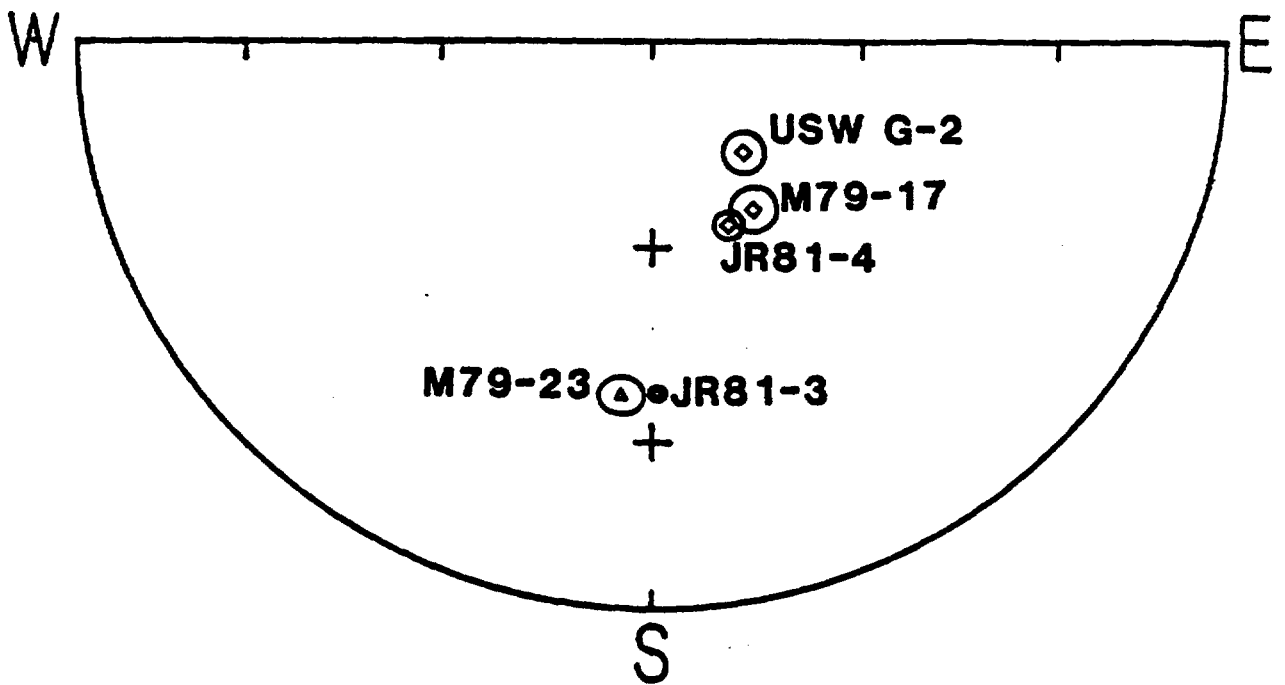


Figure 5.—Equal area projection of paleomagnetic data and associated cones of 95% confidence for the Yucca Mountain (triangles) (see Table 3) and Pah Canyon (diamonds) (see Table 4) Members of the Paintbrush Tuff.

Table 5. Magnetic Property data for the Yucca Mountain Member

Site	N	$J_{NRM}$	Sus.	Q	$D_T$	$I_T$	$J_T$	Comments
M79-23	7	.062±.006	---	---	184**	-37**	---	No susceptibility data.
JR81-3	8	.247±.029	5.54±0.18	1.08	175	-15	.153±.025	
USW G-2	15	.380±.293	4.49±2.24	1.89	170	1	.242±.242	Assumed $D_R=180^\circ$ .

For explanation of headings see Table 2. \*\* indicates remanent directions given because susceptibilities not measured.

Table 6. Magnetic Property data for the Pah Canyon Member

Site	N	$J_{NRM}$	Sus.	Q	$D_T$	$I_T$	$J_T$	Comments
M79-17	6	$2.43 \pm 1.28$	$4.35 \pm 2.31$	17.4	137	-64	$2.25 \pm 1.23$	
JRB1-4	7	$3.27 \pm 1.02$	$6.33 \pm 0.48$	12.5	171	-62	$3.14 \pm 1.02$	
USW G-2	33	$1.79 \pm 0.83$	$4.80 \pm 1.47$	8.54	154	-62	$1.60 \pm 0.78$	Assumed $D_R = 160^\circ$ .

For explanation of headings see Table 2.

**Topopah Spring Member:** The Topopah Spring Member was sampled at four outcrop localities (Figure 1) and in drill holes USW G-1, G-2, GU-3, H-1, UE25a-4, -5, -6, and -7 (Table 7).

Data from drill holes USW G-1, G-2 and GU-3 and from outcrop sampling at Busted Butte have demonstrated large changes in remanent directions with depth within the Topopah Spring Member (Figures 6a, 6b, 6c and 7). These directional variations make structural interpretations based upon differences in remanent directions of the Topopah Spring Member, such as those observed between samples from drill holes UE25a-4, -5, -6, and -7 (Figure 6d) [Spengler and Rosenbaum, 1980], tenuous at best. The reason for these changes is not clear. The directional variations may be due to changes in the magnetic field during cooling of the ash-flow sheet. Alternatively, they could be produced by internal deformation of the sheet by postemplacement flow at temperatures below which the magnetization was acquired. This latter possibility is consistent with the observation that inclinations decrease with depth from values near the expected axial dipole inclination, to values as low as 20°, and then increase sharply near the bottom of the unit (Figure 7). The shallow inclinations could be due to a process similar to that which produces an "inclination error" in sediments [King, 1955]. In this case rotation of the magnetic grains would presumably take place during the welding process. This hypothesized mechanism would require some of the welding to have occurred at temperatures below those at which the magnetization was blocked (i.e. over a range of temperatures below the Curie temperature of about 575° C). The steepening of inclinations below the bottom of the basal vitrophyre (at depths of 409 m, 508 m, and 387 m in drill holes USW G-1, G-2, and GU-3, respectively) may be related to a lessening of the amount of grain rotation with a decrease in welding toward the base of the ash-flow sheet. In contrast, because there is little variation in the degree of welding in the 200 m of tuff overlying the basal vitrophyre (all moderately to densely welded), progressive flattening of the remanence vector with depth would require a systematic variation in the proportion of grain rotations that occurred before and after blocking of the remanence. Horizontal shearing accompanying the compactional process would cause a bias in the direction of grain rotation and thereby cause changes in the declination of remanence.

It should be noted that some of the observed directional variation may be due to rotation of blocks in proximity to faults. For example, the sample from a depth of 397 m (1302.5 ft) in USW G-2 (Figure 7) which has an inclination in excess of 80° occurs in a zone of shear fractures (396.2-398.4 m) [Maldonado and Koether, 1983]. In addition it is worth noting that the direction from one sampling site outside of the Yucca Mountain block, M79-10, is nearly 20° steeper than any of the site means from Yucca Mountain and about 12° greater than the most steeply inclined data from the drill holes (Figure 6e and Table 7). This suggests some relative rotation between the Yucca Mountain block and site M79-10.

Table 7. Directional data for the Topopah Spring Member

Site	Lat.	Long.	N	D <sub>R</sub>	I <sub>R</sub>	ags	K	af	Comments
M79-10	36.772	116.316	6	304.0	75.3	2.0	1141.0	20	North end of Little Skull Mountain. Jackass Flats Quadrangle.
M79-30	36.816	116.413	7	288.2	53.6	4.2	209.2	20	
JR81-9	36.824	116.459	7	297.5	53.4	2.6	543.8	20	
Busted Butte	36.778	116.417	96	313.7	56.6	2.2	44.0	20	Southeast side of Busted Butte. Topopah Spring SW Quadrangle.
USW G-1	36.867	116.458	22	309.6	57.0	8.8	13.4	10	All oriented specimens.
			9	282.4	57.0	5.4	92.5	10	Depth 194.0-200.0 m.
			6	292.1	46.4	1.6	1858.2	10	Depth 221.5-225.0 m.
			7	359.7	49.7	4.7	164.3	10	Depth 356.0-359.0 m.
USW G-2	36.890	116.459	28	308.4	46.6	5.4	26.4	10	All oriented specimens (except depth interval 490.0-495.0 m).
			6	302.4	57.5	4.2	255.8	10	Depth 237.0-241.0 m.
			6	301.1	54.4	3.1	482.3	10	Depth 283.5-289.0 m.
			7	332.7	44.8	7.0	74.8	10	Depth 405.0-409.5 m.
			9	299.0	32.5	5.0	108.4	10	Depth 456.5-462.0 m.
			6	108.5	25.4	6.5	107.2	10	Depth 490.0-495.0 m. Core rug apparently misoriented by 180°
			6	286.6	21.3	6.5	108.5	10	Depth 490.0-495.0 m. Corrected for apparent 180° error in orientation.
USW GU-3	36.818	116.467	15	308.7	50.5	7.9	24.2	10	All oriented specimens.
			5	310.6	63.2	4.0	372.2	10	Depth 162.0-164.5 m.
			4	323.6	60.0	2.3	1655.7	10	Depth 214.5-216.5 m.
			6	301.9	32.6	5.8	135.2	10	Depth 356.0-360.0 m.
USW H-1	36.866	116.453	12	320.7	51.8	1.6	693.4	10	Depth 136.5-144.0 m.
UE25a-4	36.860	116.448	16	301.2	45.1	3.2	130.0	20	Depth 112.0-151.5 m.
UE25a-5	36.857	116.445	16	290.3	54.0	1.6	504.2	20	Depth 85.0-129.5 m.
UE25a-6	36.854	116.446	12	335.3	52.7	5.1	73.6	20	Depth 85.5-122.0 m.
UE25a-7	36.855	116.453	12	301.1	46.2	4.3	102.7	20	Depth 114.0-146.0 m.

For explanation of headings see Table 1.

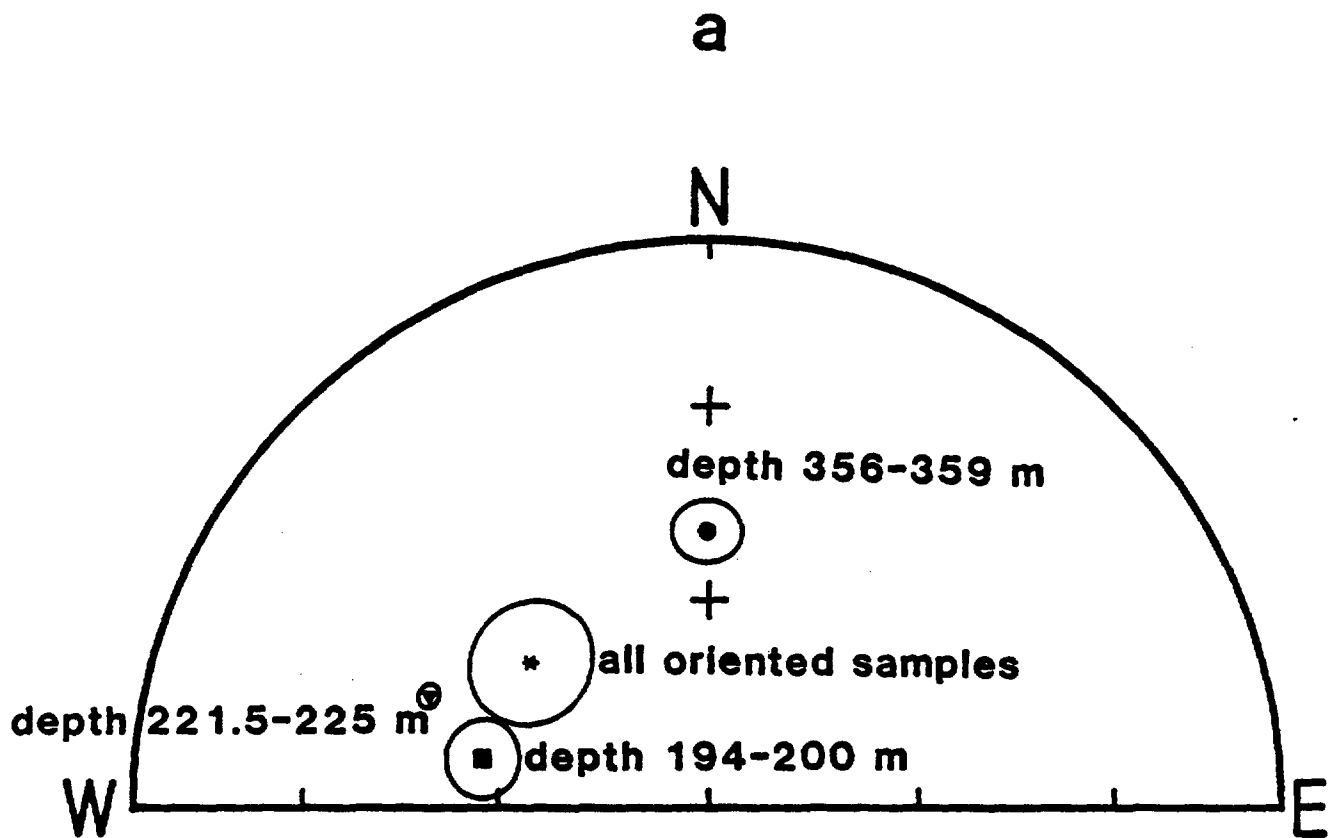


Figure 6.—Equal area projection of paleomagnetic data and associated cones of 95% confidence for the Topopah Spring Member of the Paintbrush Tuff (see Table 7): a) Drill hole USW G-1; b) Drill hole USW G-2; c) Drill Hole USW G-3; d) Drill holes UE25a-4, -5, -6, -7, and USW H-1; e) Outcrop sampling localities.

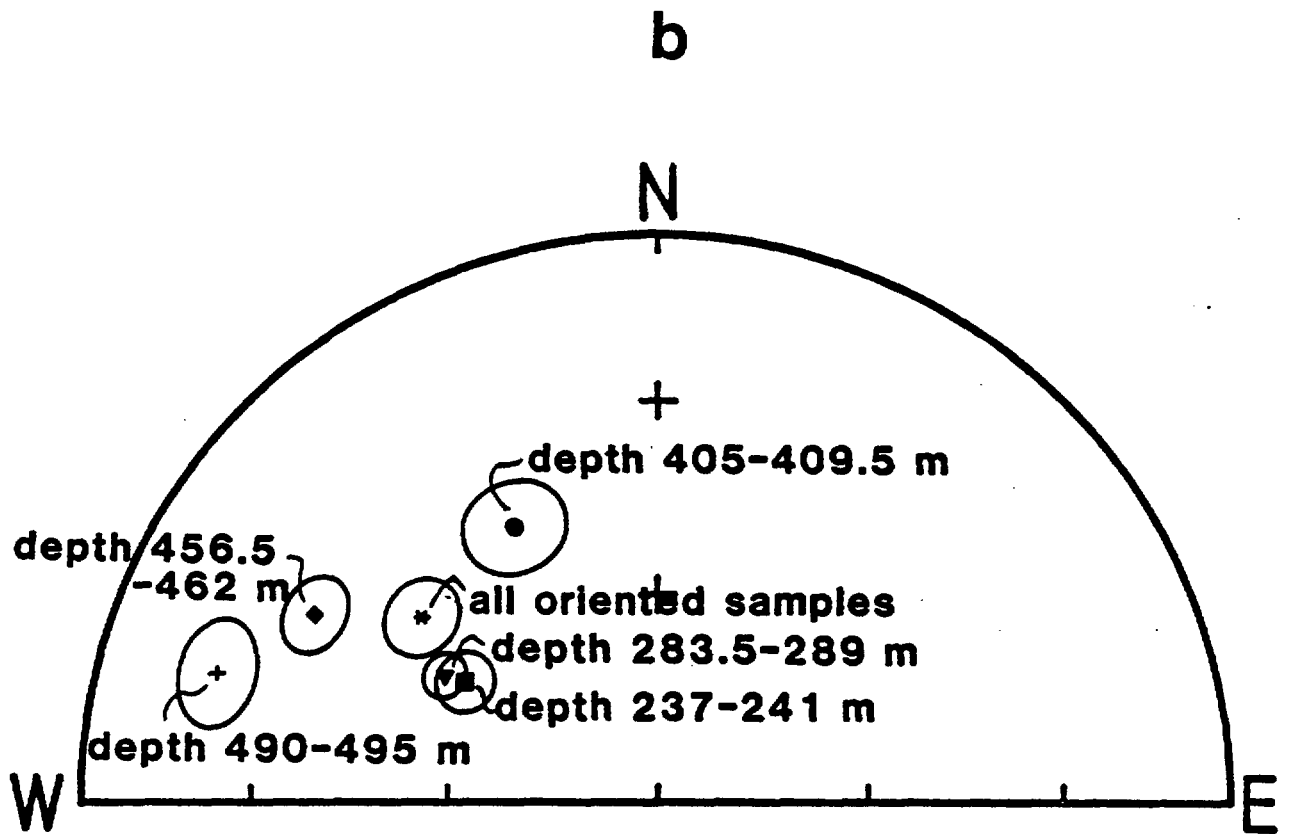


Figure 6.--continued

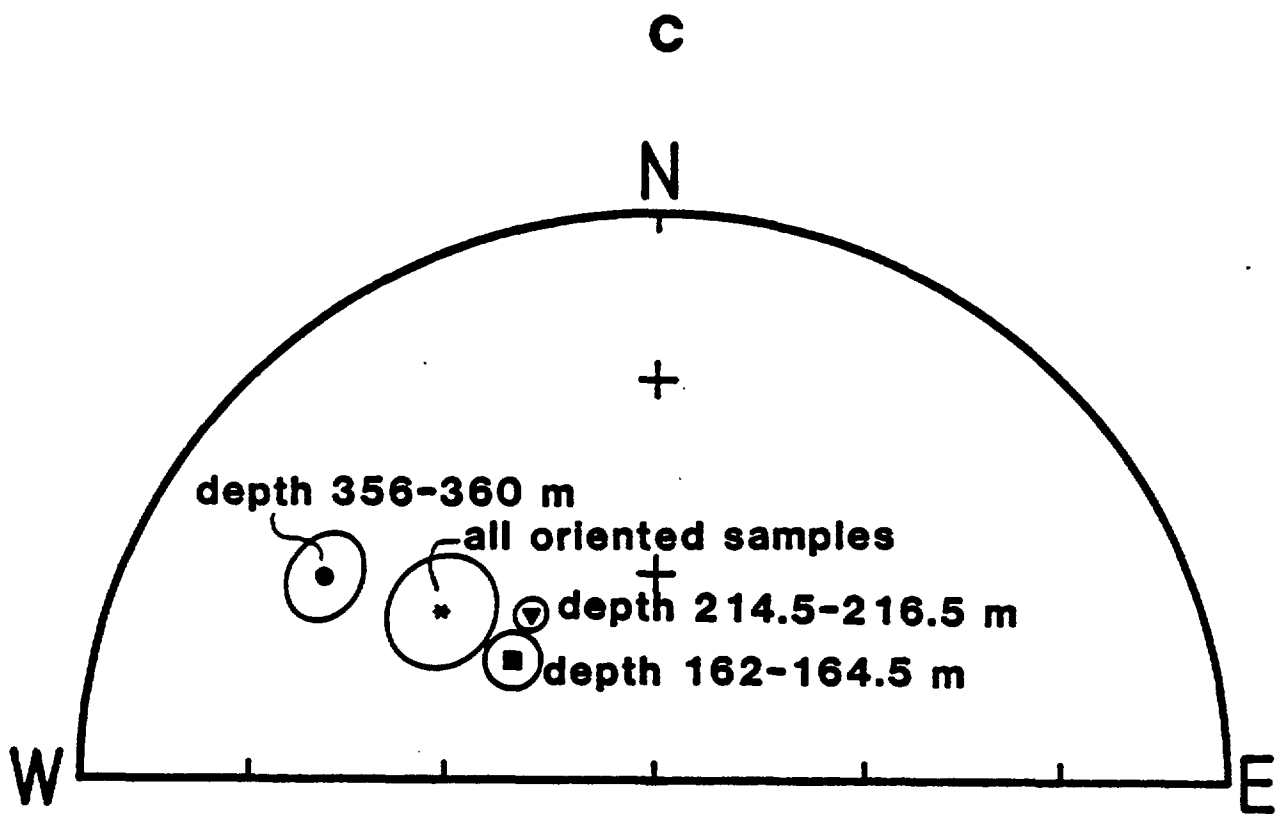


Figure 6.—continued

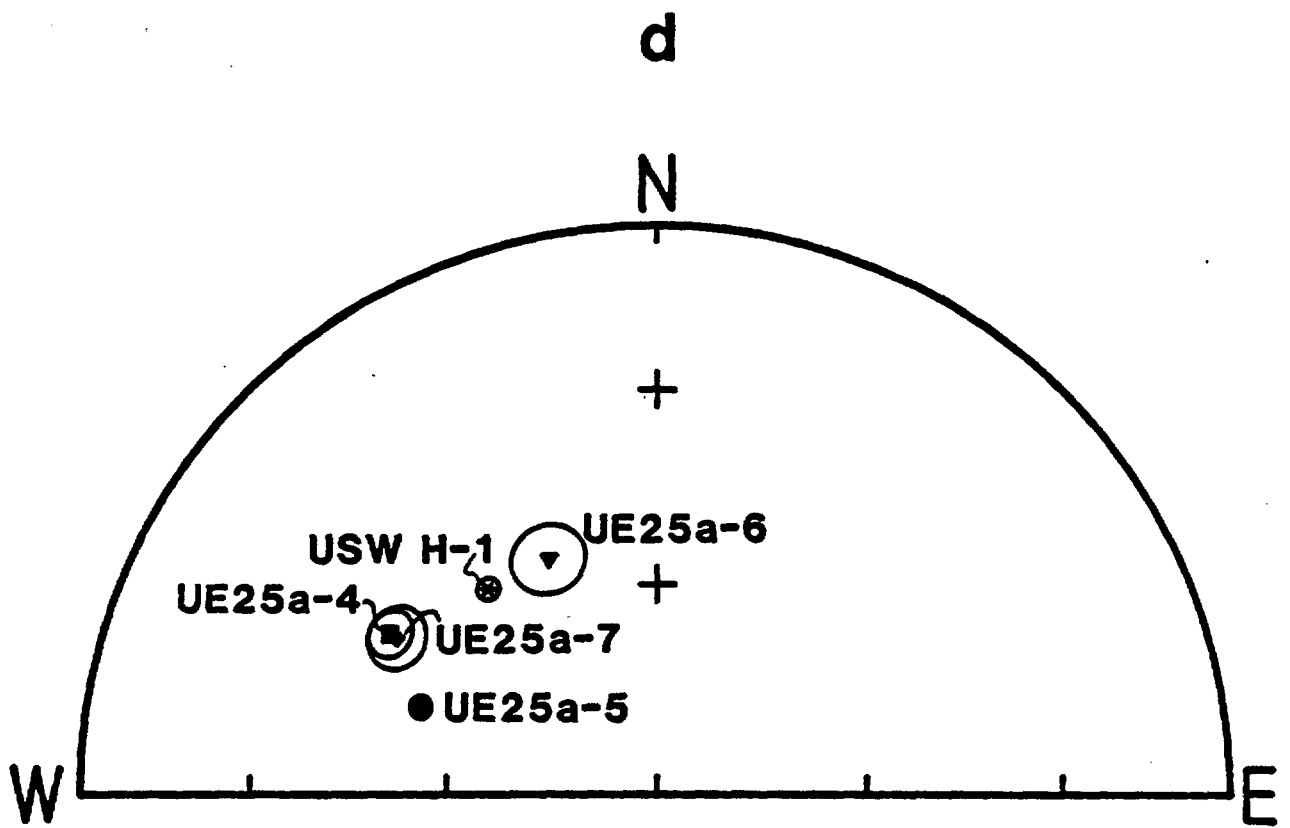


Figure 6.—continued

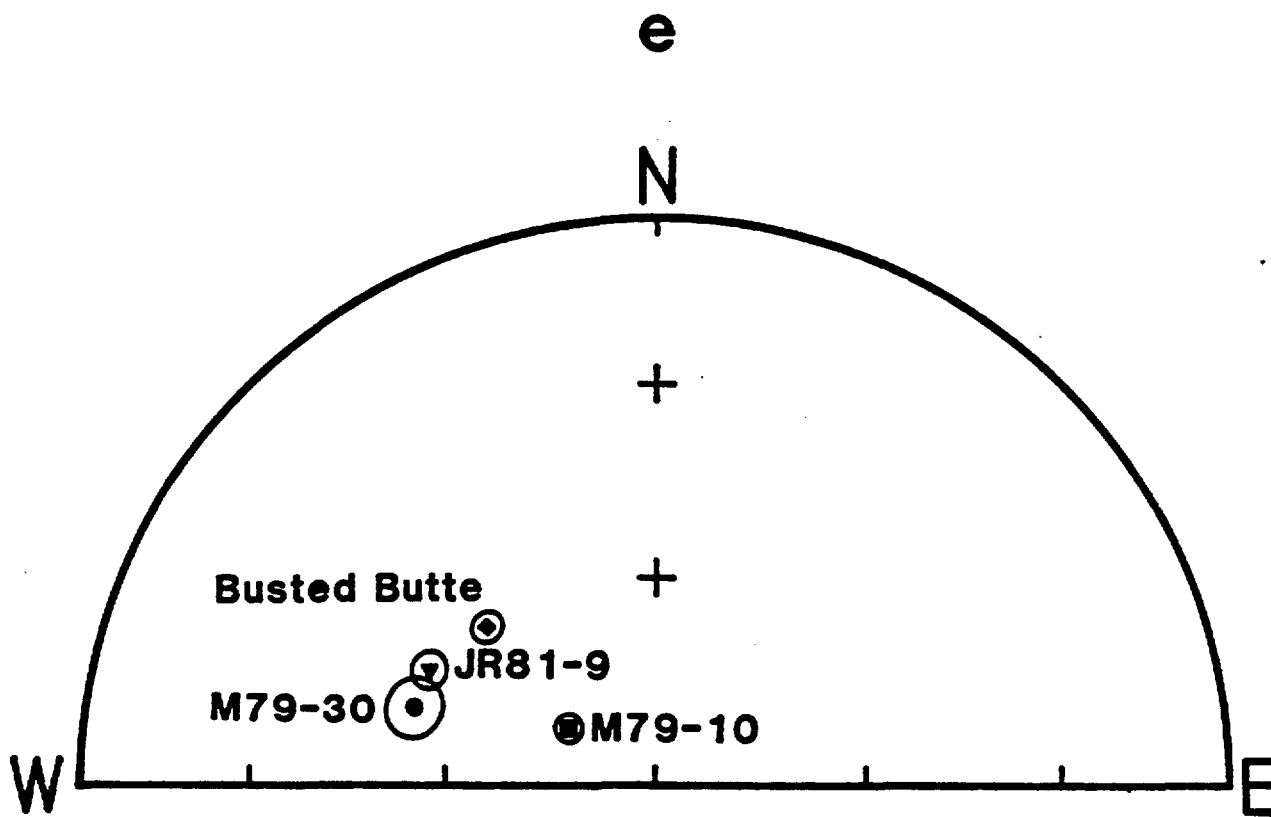


Figure 6.—continued

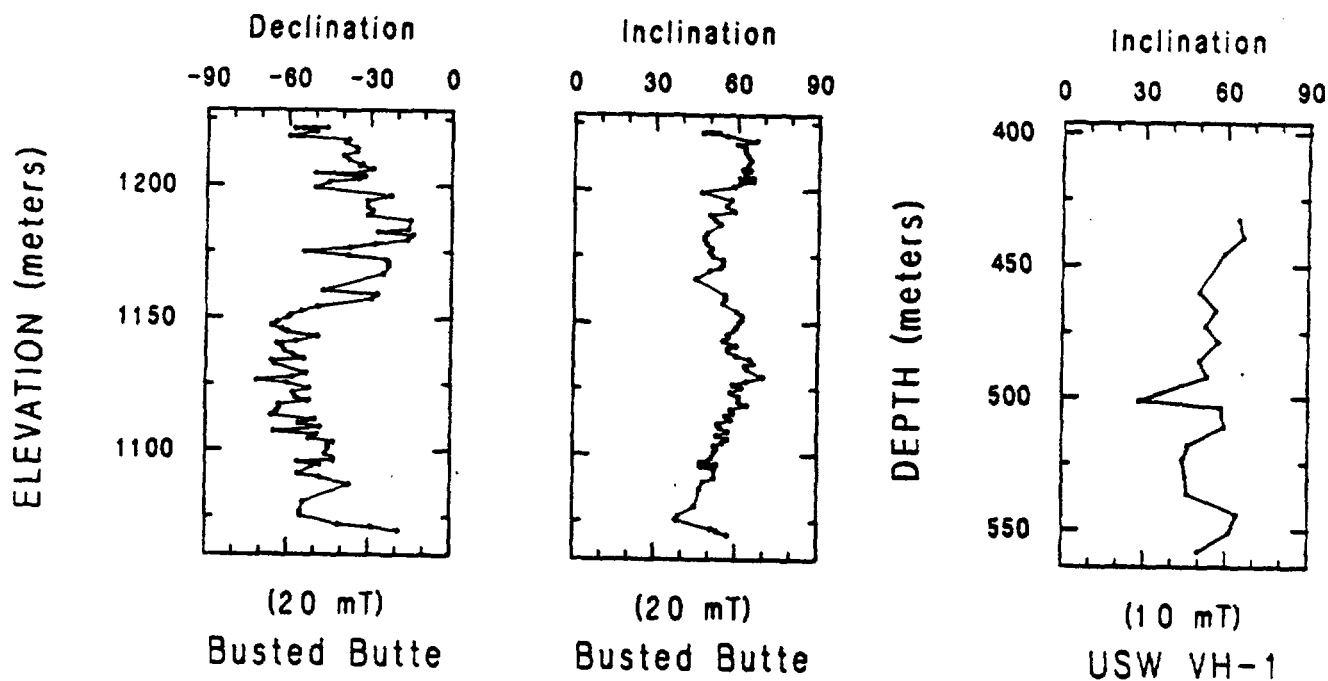
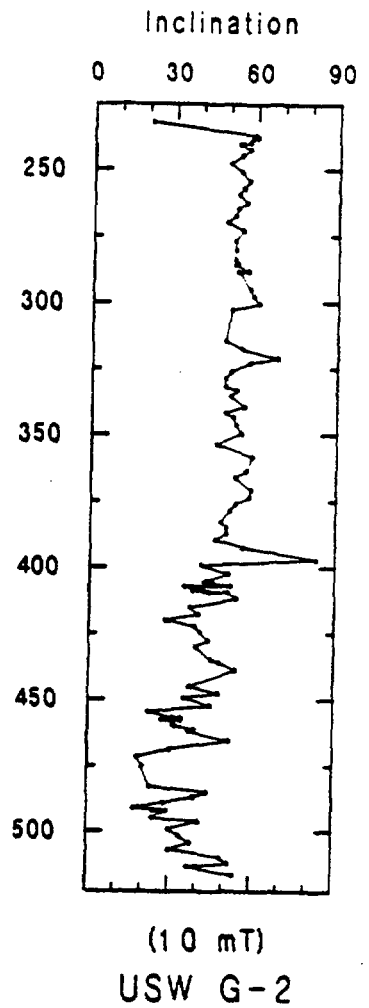
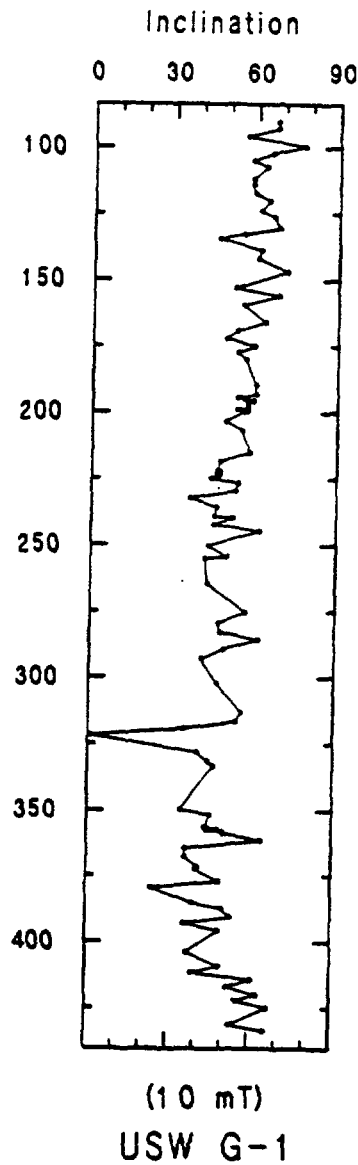
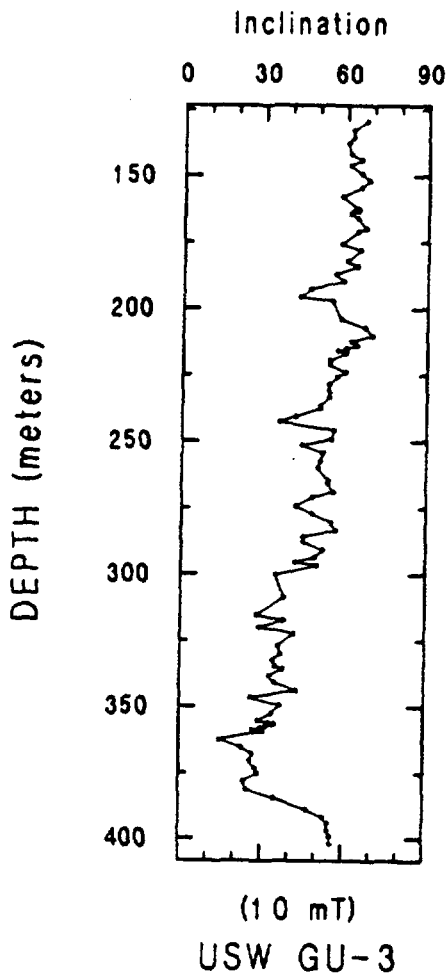


Figure 7.—Paleomagnetic data versus depth for the Topopah Spring Member of the Paintbrush Tuff; inclinations and declinations from Busted Butte after a demagnetization at a peak field of 20 mT, and inclinations



from drill hole USW VH-1, GU-3, G-1, and G-2 after af demagnetization at a peak field of 10 mT. Elevations for the Busted Butte locality were obtained by hand leveling.

Magnetization and susceptibility data for the Topopah Spring Member were obtained from throughout the unit from drill holes USW G-1, G-2, and GU-3 and from outcrop at Busted Butte. In addition the lower part of the unit was sampled from drill hole USW VH-1 (Figure 8 and Table 8). Both remanent intensity and susceptibility display large changes with depth. In some parts of the sampled sections there appears to be a high degree of correlation between these parameters; for example, between about 285 and 390 m in USW G-1, intensity and susceptibility change in a very similar manner. In other cases, such as throughout the entire section at Busted Butte and at USW GU-3, there appears to be little if any correlation between changes in susceptibility and intensity.

The only obvious correspondence between magnetic properties and gross lithology [Spengler and others, 1981; Maldonado and Koether, 1983; Scott and Castellanos, 1984] is that the basal vitrophyre correlates with a relative susceptibility minimum (vitrophyre extends between depths of about 392-409 m, 498-509 m, and 362-387 m in USW G-1, G-2 and GU-3, respectively; and between elevations of about 1090 and 1078 m at Busted Butte). In general the intensity of magnetization increases gradually with depth to the vicinity of the basal vitrophyre and then decreases sharply. Superimposed on this general trend are a number of relative maxima and minima. At Busted Butte a relative intensity maximum occurs in the basal vitrophyre. This is similar to the occurrence of an intensity peak in the basal vitrophyre of the Tiva Canyon Member in drill hole USW GU-3 (Figure 4). However, pronounced intensity maxima do not occur in the basal vitrophyre from the drill holes. In these localities the vitrophyre occurs in the zone of decreasing intensity near the base of the unit.

The reasons for the changes in magnetization and susceptibility are unknown but are probably a combination of (1) concentration of magnetite either by settling in the magma chamber or during emplacement of an ash flow, (2) post-emplacement growth of magnetic phases, and (3) oxidation of magnetite either during cooling or at low temperature. Until much more closely spaced vertical sections can be sampled, meaningful correlation of features within the sections is impossible.

Table 8. Magnetic Property data for the Topopah Spring Member

Site	N	J <sub>NRM</sub>	Sus.	Q	D <sub>T</sub>	I <sub>T</sub>	J <sub>T</sub>	Comments
M79-10	6	.156±.024	1.11	3.41	313	76	.194±.020	
M79-30	7	1.26±.981	---	---	276 <sup>**</sup>	47 <sup>**</sup>	---	No susceptibility data.
JR81-9	7	.809±.315	3.12±1.68	6.76	300	55	.862±.346	
Busted Butte	96	1.23±0.84	4.70±2.55	7.89	325	60	1.31±0.86	
USW G-1	104	1.15±1.11	3.72±2.31	10.2	322	55	1.29±1.14	Assumed D <sub>R</sub> =315°.
USW G-2	119	1.26±0.93	4.05±2.00	9.7	321	49	1.39±0.93	Assumed D <sub>R</sub> =315°.
USW GU-3	108	1.01±.541	5.25±2.22	5.38	323	53	1.19±.567	Assumed D <sub>R</sub> =315°.
USW H-1	12	.639±.088	---	---	321 <sup>**</sup>	53 <sup>**</sup>	---	Depth 136.5-144.0 m. No susceptibility data. Sample volume assumed =11.9 cm <sup>3</sup> .
VH-1	19	.681±.421	4.88±1.81	3.37	328	59	.858±.455	Depth 432.5-558.0 m. Assumed D <sub>R</sub> =315°.
UE25a-4	26	.461±.115	4.96±1.09	2.30	312	50	.543±.125	Depth 112.0-151.5 m.
UE25a-5	19	.645±.625	4.94±2.22	3.10	298	55	.723±.64	Depth 85.0-129.5 m.
	18	.503±.083	4.51±1.24	2.93	298	56	.576±.085	Depth 101.5-129.5 m. Same data with highly magnetic sample at 85.3 m deleted.
UE25a-6	13	.458±.154	4.80±1.28	2.37	339	58	.549±.169	Depth 85.5-122.0 m.
UE25a-7	15	.488±.077	4.27±0.97	2.88	309	51	.558±.079	Depth 114.0-146.0 m.

For explanation of headings see Table 2. <sup>\*\*</sup> indicates remanent directions given because susceptibilities not measured.

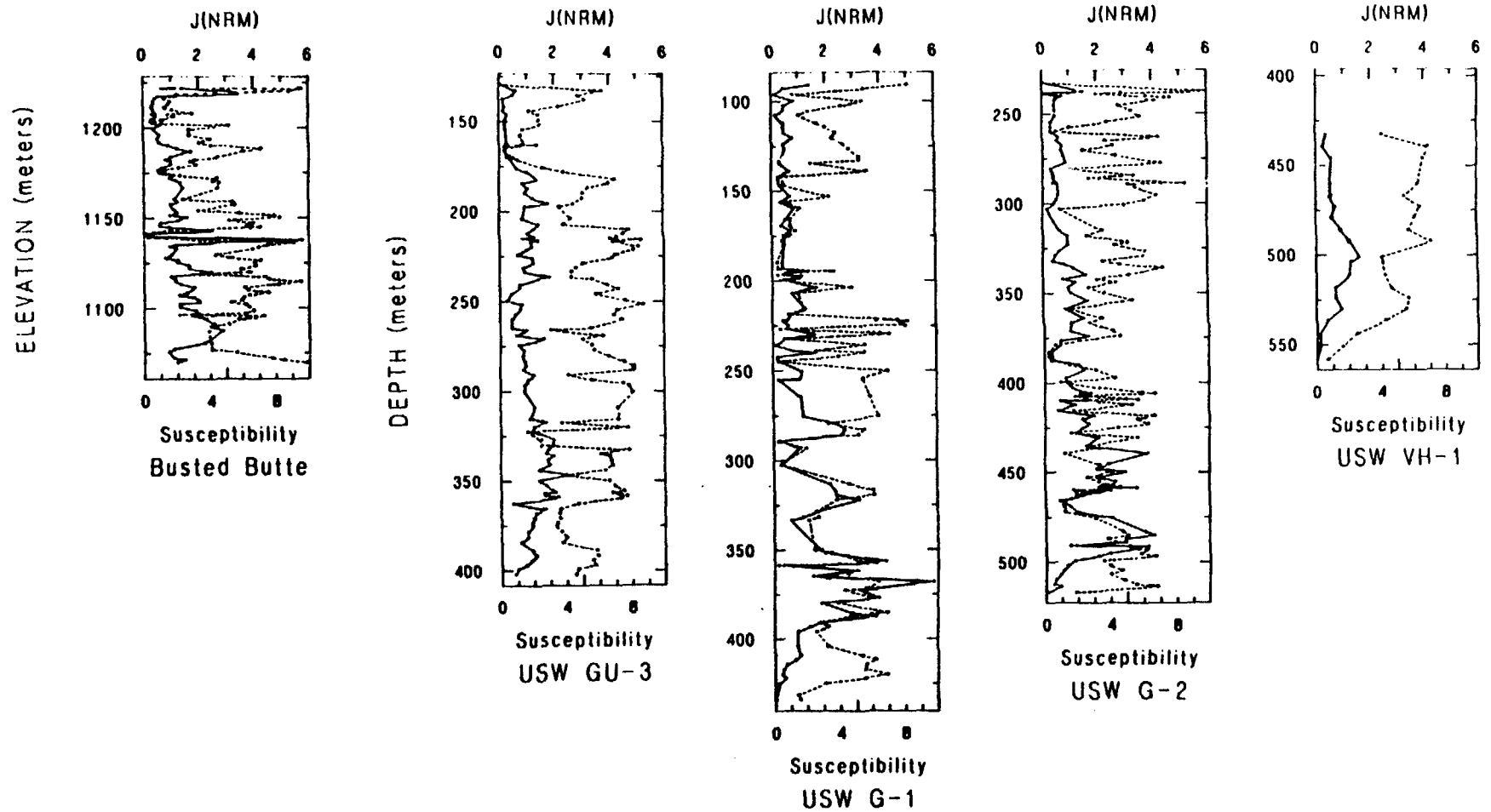


Figure 8.—Intensity of natural remanent magnetization,  $J(\text{NRM})$ , in  $\text{Am}^{-1}$  (circles and solid line) and SI susceptibility  $\times 10^3$  (squares and dashed line) for the Topopah Spring Member of the Paintbrush Tuff. Elevations for the Busted Butte locality were obtained by hand leveling.

### Tuffaceous beds of Calico Hills

The tuffaceous beds of Calico Hills, a sequence of ash-flow tuffs and thin reworked tuffs, was sampled in drill holes USW G-1 and G-2. The only oriented specimens were obtained from a depth interval between 466.5 and 468.5 m in USW G-1 near the base of a 34.5 m thick ash-flow tuff [Spengler and others, 1981]. After af demagnetization to 20 mT these samples yield a mean direction of  $D=337.1^\circ$ ,  $I=67.5^\circ$  ( $\alpha_{95}=10.7$ ,  $K=39.9$ ).

The inclination data are quite noisy, with many of the spikes being within reworked tuff intervals and the margins of various ash-flow tuffs. Nevertheless, inclination data from both USW G-1 and G-2 show consistent patterns (Figure 9). Inclinations increase from about  $40^\circ$  in the lowermost ash-flow tuff in USW G-1 (base of this tuff is at a depth of about 529 m) to values of about  $70^\circ$  near the top of the Calico Hills at this locality. Inclinations from the basal ash-flow tuff in USW G-2 are also about  $40^\circ$ . Remanent directions then steepen to about  $70^\circ$  (or more) in the depth interval 720-775 m, and then flatten with decreasing depth to about  $30^\circ$  in the upper part of the unit. These patterns suggest that the ash-flow tuffs which comprise the Calico Hills were erupted over a long period relative to changes in the direction of the earth's magnetic field (secular variation). These patterns also indicate that the section present in drill hole USW G-1 is correlative with no more than the lowermost 100-125m of the section encountered in USW G-2.

The ash-flow and bedded tuffs of the Calico Hills, sampled in drill holes USW G-1 and G-2, have maximum intensities of remanent magnetization of about  $0.5 \text{ Am}^{-1}$  and average intensities of about  $0.1 \text{ Am}^{-1}$  or less (Figure 10 and Table 9).

In the Calico Hills from USW G-1 the highest values of magnetization and relatively high values of susceptibility occur in samples from a single ash-flow tuff which extends from a depth of 479 to 516 m (Spengler and others, 1981). In addition, a large susceptibility peak occurs in the tuffaceous sandstone which makes up the bottom 20 m of the unit at this locality.

The uppermost 75 m of the Calico Hills from drill hole USW G-2 contains magnetization and susceptibility maxima with peak values similar to those in the central part of the unit at USW G-1 (Figure 10). However, the upper 75 m of the unit from USW G-2 comprises five ash flows each less than 16 m in thickness, while the maxima from USW G-1 occur in a single flow about 37 m thick (Spengler and others, 1981; Maldonado and Koether, 1983). If the proposed correlation (based on paleomagnetic inclinations) between these two sections is correct, then the 37 m thick, relatively magnetic tuff from USW G-1 can correspond to nothing above a depth of 785 m in USW G-2. Possibly this ash-flow tuff in USW G-1 corresponds to a lower part of the Calico Hills section which has been removed by faulting at USW G-2 [Maldonado and Koether, 1983].

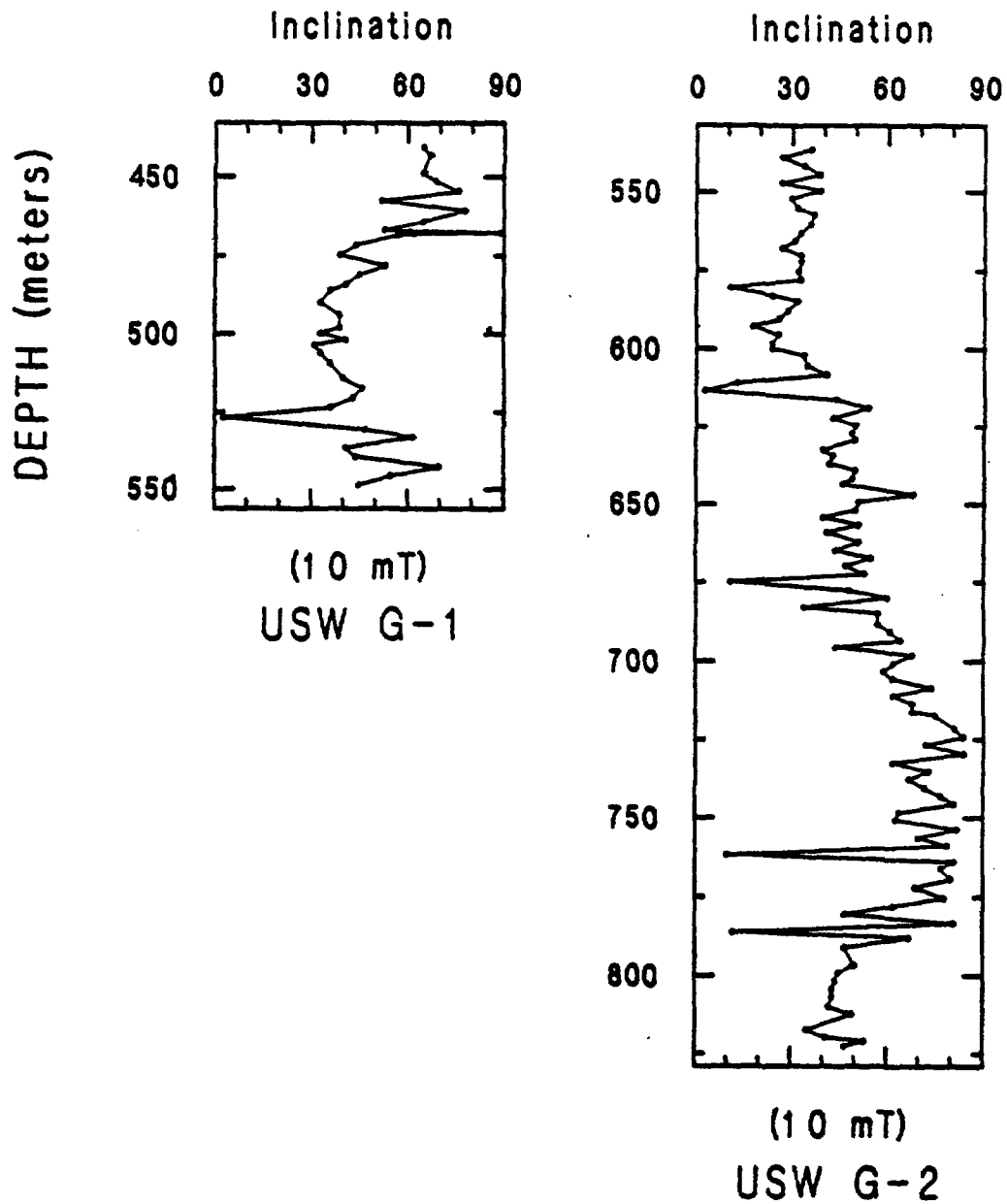


Figure 9.—Paleomagnetic inclinations versus depth for the tuffaceous beds of Calico Hills after af demagnetization at a peak field of 10 mT.

Table 9. Magnetic Property data for the tuffaceous beds of Calico Hills

Site	N	$J_{NRM}$	Sus.	Q	$D_T$	$I_T$	$J_T$	Comments
USW G-1	42	$.102 \pm .116$	$1.55 \pm 1.46$	2.18	5	56	$.163 \pm .155$	Assumed $D_R=0^\circ$ .
USW G-2	111	$.073 \pm .118$	$0.92 \pm 1.48$	1.63	6	56	$.110 \pm .139$	Assumed $D_R=0^\circ$ .

For explanation of headings see Table 2.

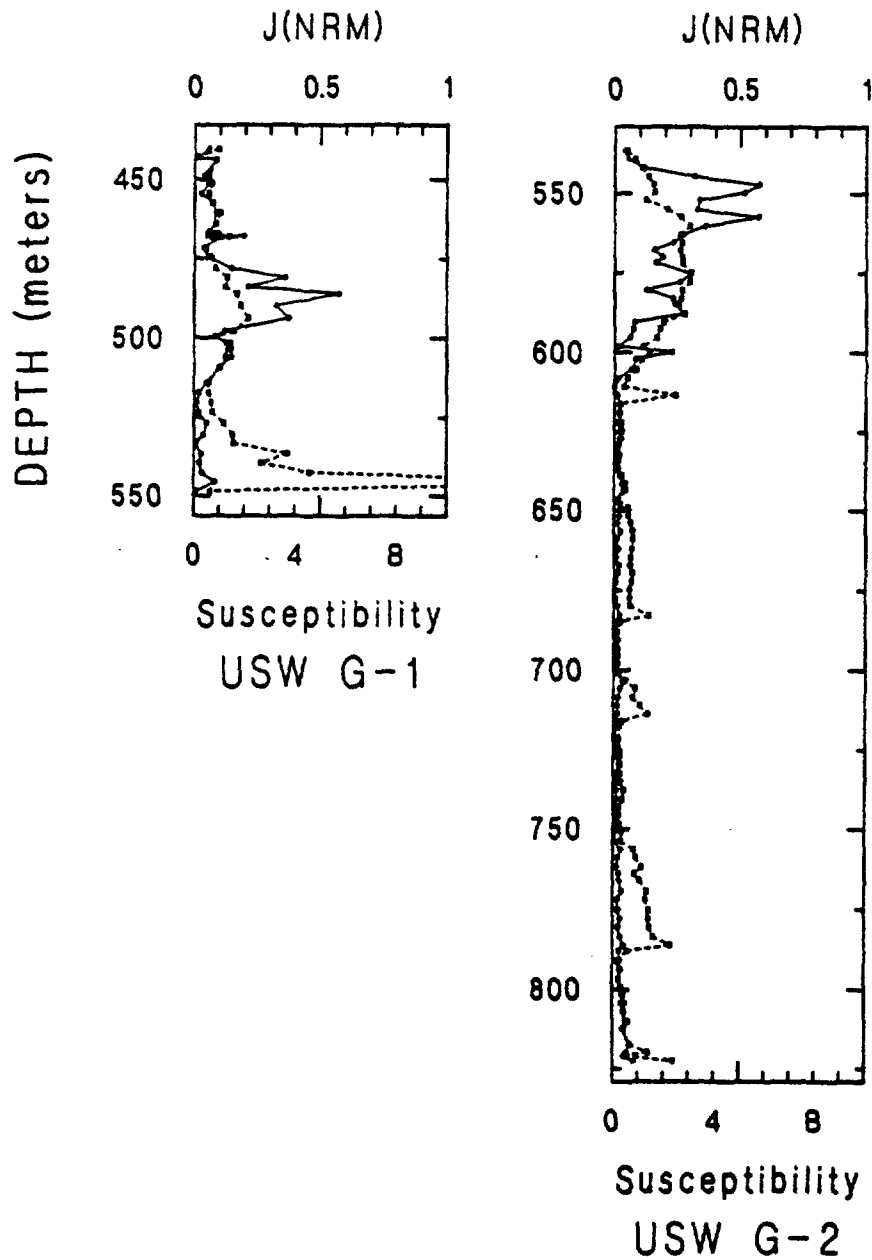


Figure 10.—Intensity of natural remanent magnetization,  $J(\text{NRM})$ , in  $\text{Am}^{-1}$  (circles and solid line) and SI susceptibility  $\times 10^3$  (squares and dashed line) for the Tuffaceous Beds of Calico Hills.

## Crater Flat Tuff

**Prow Pass Member:** The Prow Pass Member was sampled in drill holes USW G-1, G-2, GU-3 and VH-1. Mean remanent directions from the three depth intervals from which oriented core was obtained in drill hole USW G-1 differ significantly (Figure 11 and Table 10). One of these depth intervals falls in each of three subunits of the Prow Pass [Spengler and others, 1981]. Therefore it is possible that the directional variation is due to movement of the magnetic field between the times of emplacement of these subunits. However, since differences in the inclinations of the mean directions are small it is also possible that the apparent directional changes are due to misorientation of the core segments. Samples from the single depth intervals from which oriented core was obtained in USW G-2 and GU-3 yield mean remanent directions which nearly coincide with that from the 616.5-622.0 m interval in USW G-1 (Figure 11).

No large consistent changes in inclination are observed with depth (Figure 12). Three samples from USW G-1 yield apparently aberrant directions. These are the uppermost sample collected and samples at depths of 604.7 m (1883.5 ft) and 607.8 m (1893.5 ft) which fall just above and just below the contact between the upper and middle units of the Prow Pass. These high and low inclinations may be due to remagnetization during alteration of the tuff in these zones. Similarly, the highly variable inclination record below about 930 m in USW G-2 occurs in a subunit which is intensely altered (zeolitized and silicified) [Maldonado and Koether, 1983].

The remanent intensity of the Prow Pass Member averages a few tenths of an ampere per meter at three of the localities at which it was sampled (Figure 13 and Table 11). At the fourth, drill hole USW G-2, the average remanent intensity is less than  $0.1 \text{ Am}^{-1}$ . There is a general similarity in the patterns of intensity and susceptibility changes with depth between drill hole USW G-1 and GU-3. The uppermost part of the unit at these localities is characterized by relatively high intensities (including the only values greater than  $1 \text{ Am}^{-1}$ ) and susceptibilities. Values for both of these parameters decrease with depth; still deeper susceptibility increases while magnetization remains quite low. The variations of magnetization and susceptibility with depth observed in the section of the Prow Pass sampled in drill hole USW VH-1 are similar to the uppermost portions of those from USW G-1 and GU-3.

The intensity and susceptibility curves determined for USW G-2 bear little resemblance to those from USW G-1 and GU-3. This can be attributed to two reasons. First, the uppermost portion of the Prow Pass has been faulted out at the USW G-2 locality, and second the rock at this location (especially in the lower part of the unit) is highly altered by zeolitization and silicification [Maldonado and Koether, 1983]. During the alteration process magnetite was probably oxidized to less magnetic hematite. This would account for the very low remanent intensities observed throughout the Prow Pass Member at this location.

Table 10. Directional data for the Prow Pass Member

Site	Lat.	Long.	N	D <sub>R</sub>	I <sub>R</sub>	a <sub>95</sub>	K	af	Comments
USW G-1	36.867	116.458	18	353.5	44.6	5.9	35.7	20	All oriented specimens.
			6	330.7	44.9	4.2	256.4	20	Depth 595.0-600.5 m.
			5	355.3	46.7	2.9	700.7	20	Depth 616.5-622.0 m.
			6	9.0	38.3	3.3	419.8	20	Depth 637.5-643.5 m.
USW G-2	36.890	116.459	8	348.6	38.2	2.8	395.4	20	Depth 826.0-830.5 m.
USW GU-3	36.818	116.467	6	0.2	48.8	2.4	812.9	10	Depth 515.5-517.5 m.

For explanation of headings see Table 1.

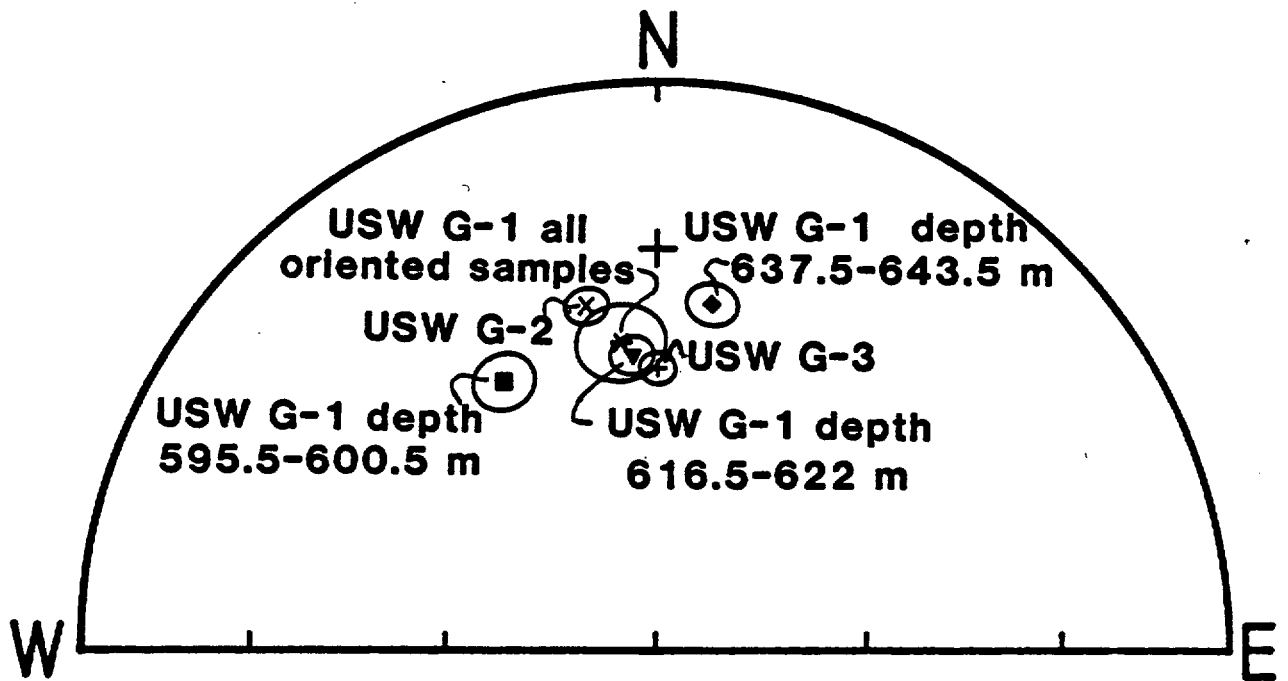


Figure 11.—Equal area projection of mean paleomagnetic directions and associated cones of 95% confidence for the Prow Pass Member of the Crater Flat Tuff (see Table 10).

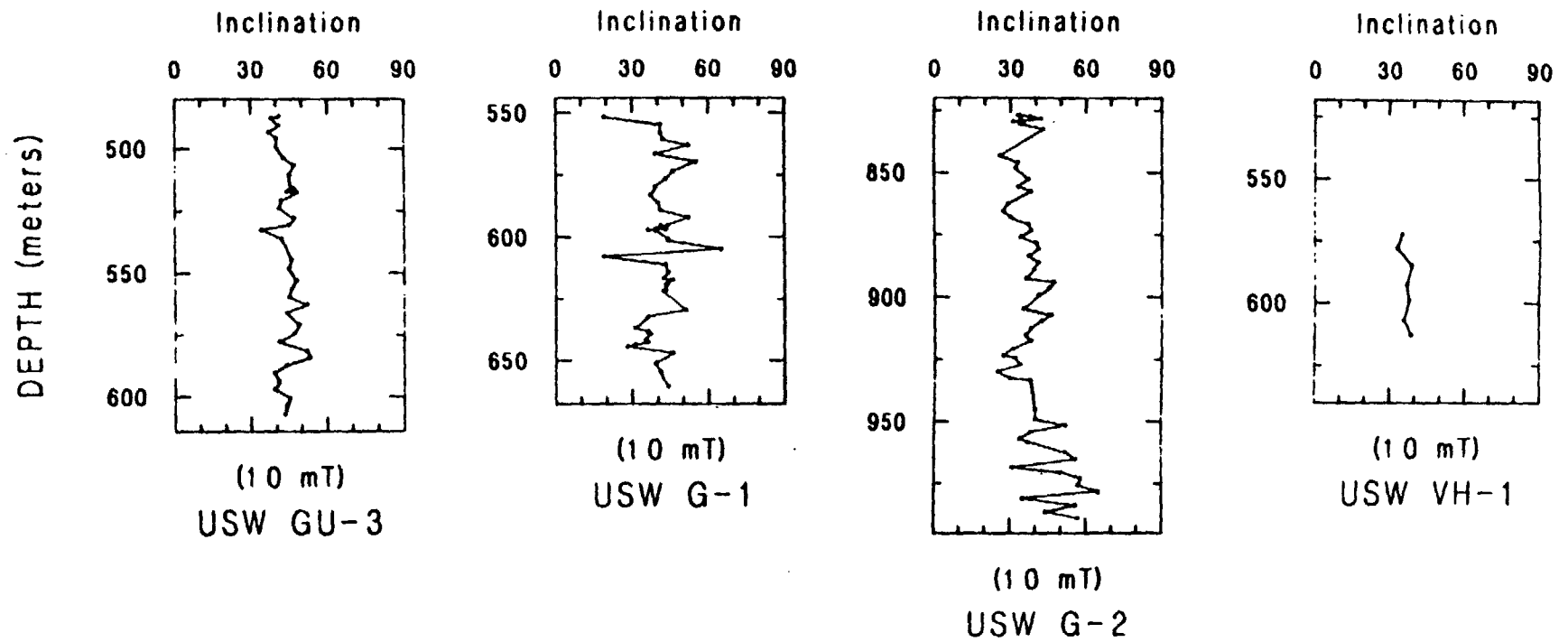


Figure 12.—Paleomagnetic inclinations versus depth for the Prow Pass Member of the Crater Flat Tuff after of demagnetization at a peak field of 10 mT.

Table 11. Magnetic Property data for the Prow Pass Member

Site	N	$J_{NRM}$	Sus.	Q	$D_T$	$I_T$	$J_T$	Comments
USM G-1	47	.287±.322	2.34±0.94	3.05	-4	50	.376±.330	Assumed $D_R=350^\circ$ .
USM G-2	62	.085±.074	1.27±1.13	1.85	-3	50	.133±.108	Assumed $D_R=350^\circ$ .
USM GU-3	40	.331±.210	1.80±1.63	19.6	4	53	.403±.232	Assumed $D_R=2^\circ$ .
VH-1	7	.524±.498	2.71±0.72	4.18	354	45	.625±.518	Assumed $D_R=350^\circ$ . Depth 572.0-643.0 m.

For explanation of headings see Table 2.

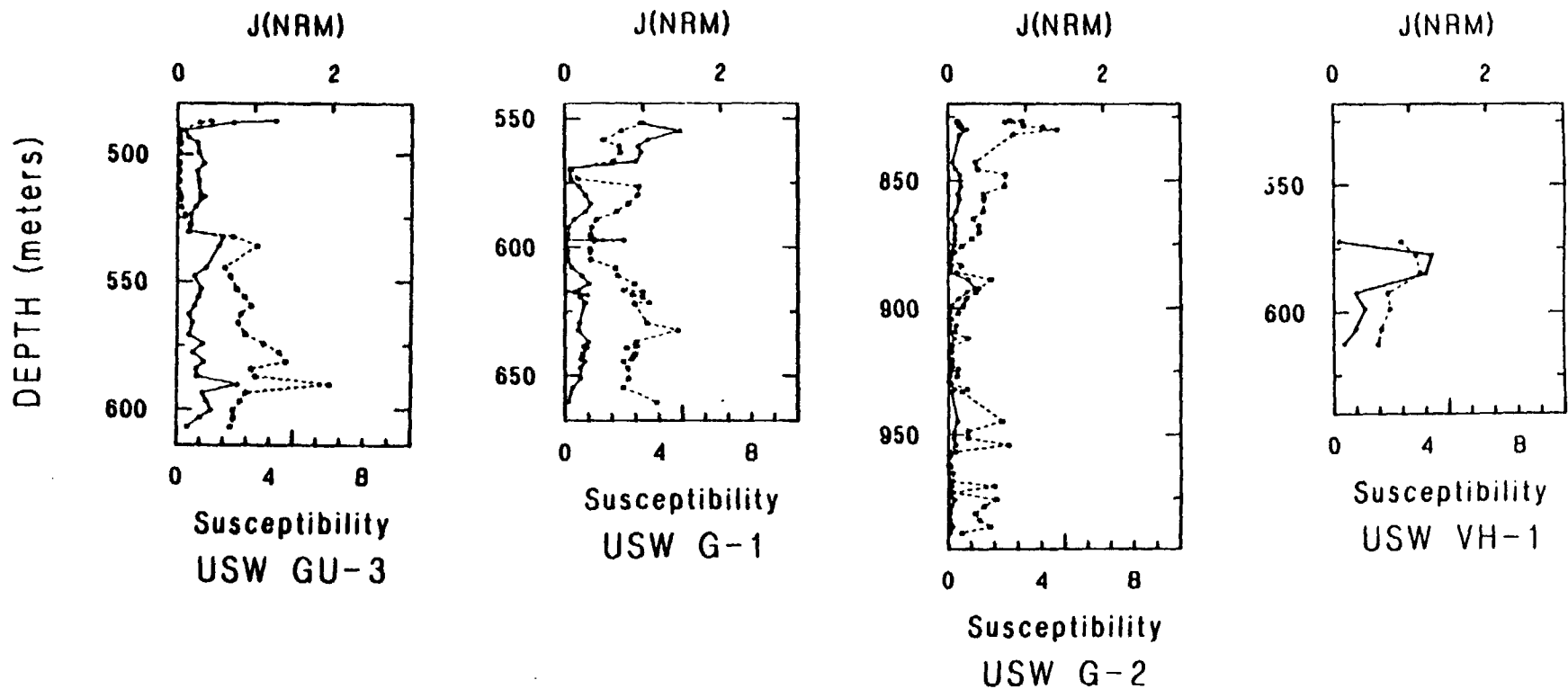


Figure 13.—Intensity of natural remanent magnetization,  $J(\text{NRM})$ , in  $\text{Am}^{-1}$  (circles and solid line) and SI susceptibility  $\times 10^3$  (squares and dashed line) for the Prow Pass Member of the Crater Flat Tuff.

**Bullfrog Member:** Oriented samples were obtained from one surface locality and drill holes USW G-1, G-2 and GU-3. Mean remanent directions from USW G-1 and GU-3 fall near that from the outcrop site (Figure 14 and Table 12). The mean direction from G-2 lies significantly to the west. Although this could be due to a tectonic rotation, or a number of other causes, perhaps the most likely explanation is an error in the orientation data.

Inclination data from drill holes USW GU-3 and VH-1 are quite uniform throughout (Figure 15). In contrast, data from USW G-2 contain relatively high inclinations near the top of the unit which may be due to alteration of the tuff in this zone. Data from USW G-1 contains two zones of extremely low inclination at about 700 m and 780 m. The low near 700 m occurs near a shear fracture [Spengler and others, 1981] and could be attributed to either rotation of rock in response to movement on the fault or to remagnetization of the rock due to alteration of the magnetic phases by fluids moving along the fracture. Similarly, the low at about 780 m occurs in a zone of fracturing.

A high degree of similarity exists between the patterns of intensity and susceptibility variation in the Bullfrog Member from drill holes USW GU-3 and VH-1 (Figure 16). Both intensity and susceptibility at these two localities define: (1) a broad minimum at a depth of about 625 m in USW GU-3 and 640 m in VH-1; (2) a maximum at about 650 m in USW GU-3 and 675 m in VH-1; and (3) a sharp minimum at 660-665 m in USW GU-3 and 690 m in VH-1. Below this the susceptibility increases and remains relatively high (mostly between 5 and 7 X  $10^{-3}$  SI) to the bottom of the moderately to densely welded portion of the unit at about 765 m in USW GU-3 [Scott and Castellanos, 1984] and to the bottom of drill hole USW VH-1. In USW GU-3 the remanent intensity curve increases below 665 m and contains a number of well defined peaks in the moderately to densely welded interior of the unit. Intensities also increase in the lower portion of the core from USW VH-1 but do not approach the amplitude of those from USW GU-3.

Of particular interest is a minimum in both magnetization and susceptibility at 777 m in USW GU-3. These minima coincide with a cooling break recognized by Scott and Castellanos [1984] on the basis of a minimum in the degree of welding and the presence of nearly a meter of bedded tuff. Similar minima in magnetization and intensity are associated with depositional breaks in the Tram Member (see below).

The average remanent intensity of the Bullfrog Member from drill hole USW G-1 is much less than that from either USW GU-3 or VH-1 (Table 13). In addition, the distinctive variations observed near the top of the unit at these latter localities are not present in the record from USW G-1. At this locality intensities gradually decrease while susceptibilities increase with depth in the upper 75 m of the unit. Below about 740 m both intensity and susceptibility increase to a maximum near the base of the moderately to densely welded portion of the flow [Spengler and others, 1981] and then fall as the degree of welding decreases near the base of the unit.

The entire thickness of the Bullfrog Member is highly altered at drill hole USW G-2 [Maldonado and Koether, 1983] and both remanent intensity and susceptibility are characterized by low values at this locality.

Table 12. Directional data for the Bullfrog Member

Site	Lat.	Long.	N	D <sub>R</sub>	I <sub>R</sub>	a <sub>95</sub>	K	af	Comments
M79-14	36.690	116.537	6	13.3	44.1	2.1	973.5	30	NE part of Big Dune Quadrangle. *
USW G-1	36.867	116.458	10	10.9	37.3	5.6	74.8	20	Depth 662.5-803.0 m.
USW G-2	36.890	116.459	8	339.4	34.4	7.8	51.2	20	Depth 1048.5-1051.5 m.
USW GU-3	36.818	116.467	7	359.0	43.8	4.3	198.2	10	Depth 725.5-798.0 m.

For explanation of headings see Table 1.

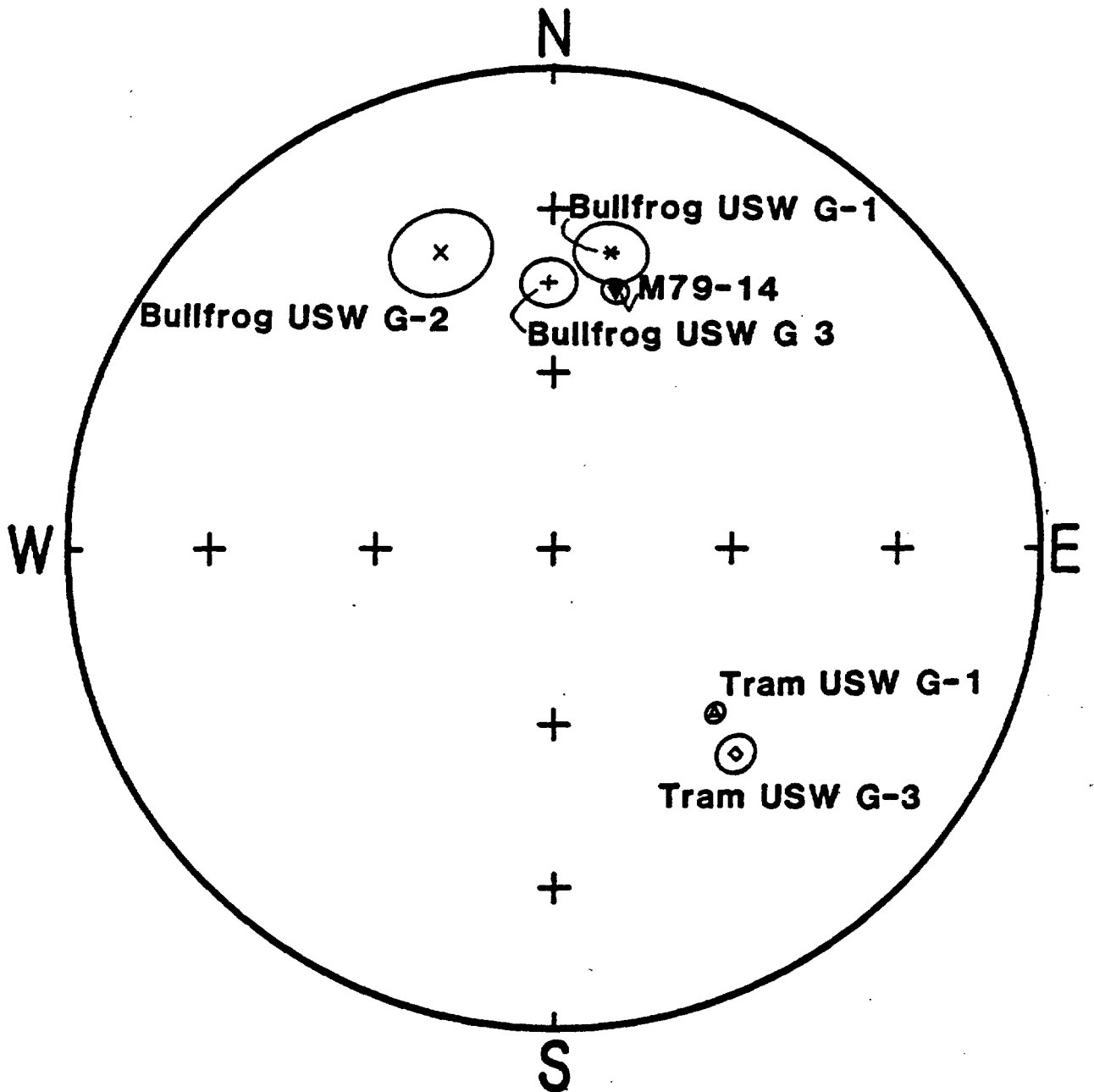


Figure 14.—Equal area projection of mean paleomagnetic directions and associated cones of 95% confidence for the Bullfrog and Tram Members of the Crater Flat Tuff (see Table 12 and 14).

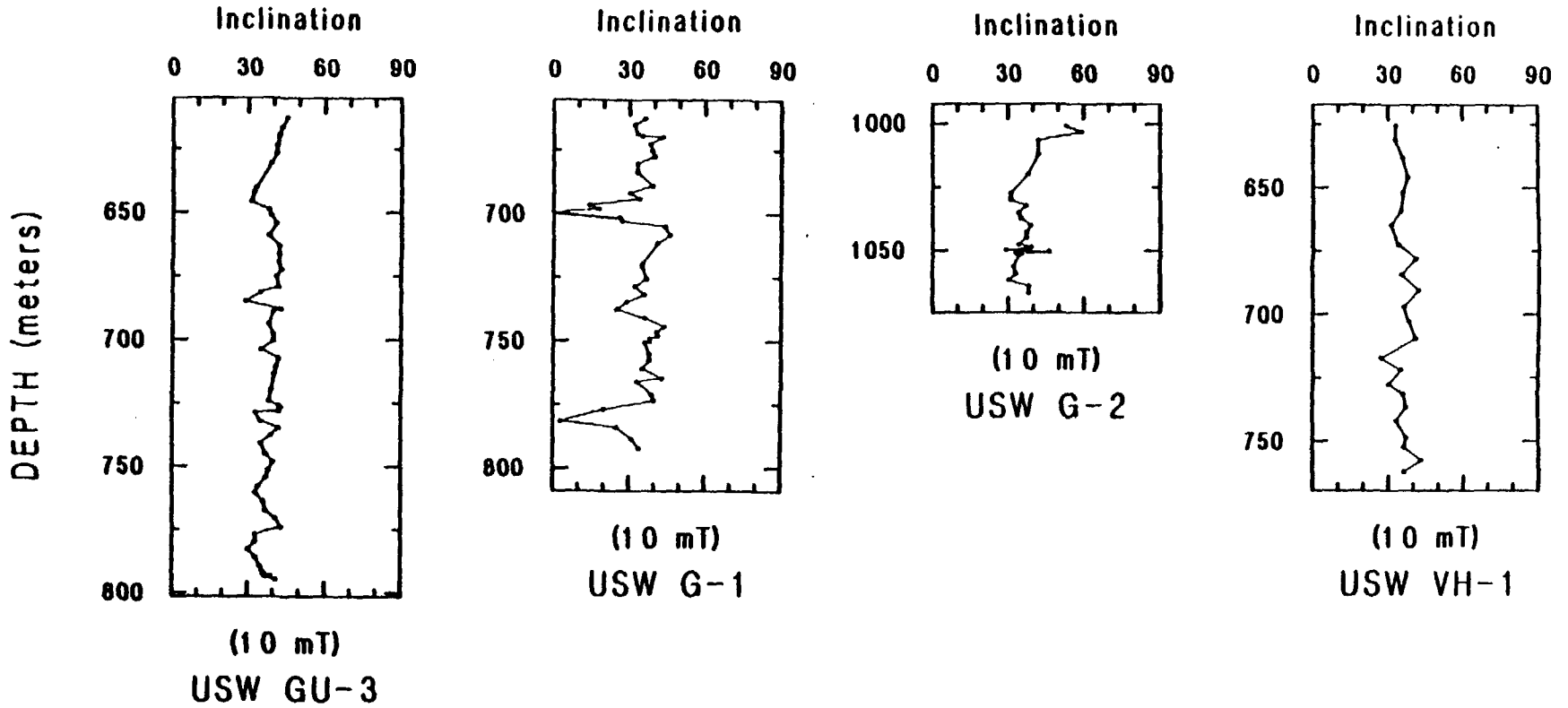


Figure 15.—Paleomagnetic inclinations versus depth for the Bullfrog Member of the Crater Flat Tuff after demagnetization at a peak field of 10 mT.

Table 13. Magnetic Property data for the Bullfrog Member

Site	N	$J_{NRM}$	Sus.	Q	$D_T$	$I_T$	$J_T$	Comments
M79-14	6	5.18±2.00	7.70±1.17	16.1	23	46	5.48±2.03	
USW G-1	47	.806±.524	3.96±1.36	5.17	12	41	.953±.549	Assumed $D_R=12^\circ$ .
USW G-2	28	.120±.098	1.02±0.84	4.60	13	49	.160±.125	Assumed $D_R=12^\circ$ .
USW GU-3	60	2.80±1.91	4.46±2.16	16.1	4	41	2.97±1.96	Assumed $D_R=3^\circ$ .
VH-1	24	1.78±1.11	4.30±2.27	11.1	12	38	1.94±1.18	Assumed $D_R=12^\circ$ . Depth 625.0-762.0 m.

For explanation of headings see Table 2.

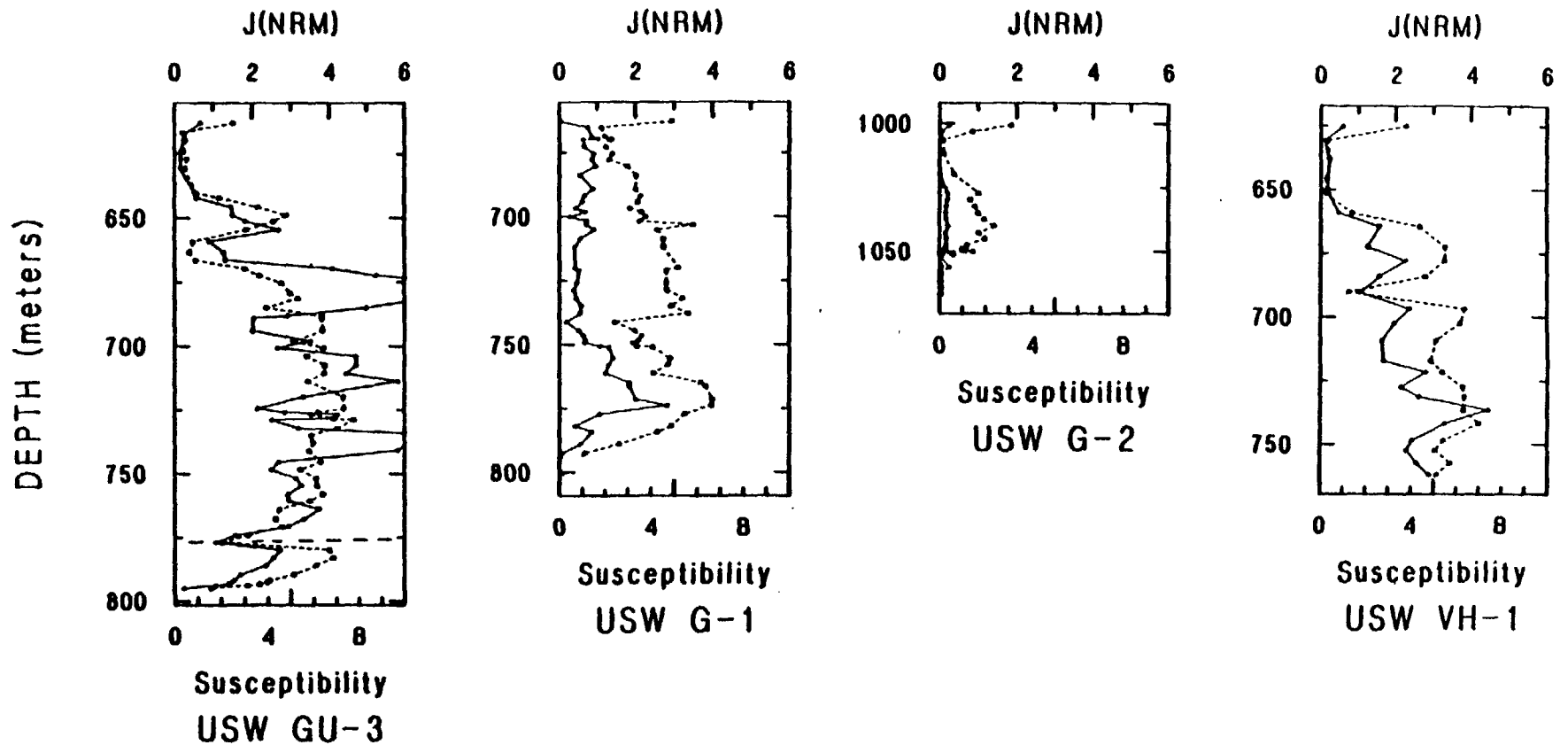


Figure 16.—Intensity of natural remanent magnetization,  $J(NRM)$ , in  $A m^{-1}$  (circles and solid line) and SI susceptibility  $\times 10^3$  (squares and dashed line) for the Bullfrog Member of the Crater Flat Tuff. Horizontal dashed line in plot of USW GU-3 data represents a depositional break [Scott and Castellanos, 1984].

**Tram Member:** The Tram Member was sampled in drill holes USW G-1, G-2 and G-3. At Yucca Mountain the Tram can be divided into upper (lithic-poor) and lower (lithic-rich) zones. Both zones occur in holes USW G-1 and G-3, but only the lithic-rich zone occurs in USW G-2 [Spengler and others, 1981; Maldonado and Koether, 1983; Scott and Castellanos, 1984].

Oriented specimens obtained from USW G-1 and G-3 yield reversed directions with south-easterly declinations (Figure 14 and Table 14). Although the data from USW G-1 give a smaller  $\alpha_{95}$  and larger precision parameter than those from USW G-3, it is likely that the G-3 data is more representative since the number of samples and the stratigraphic interval sampled are much greater for this hole than for USW G-1.

Inclination data for the Tram Member from USW G-3 remain quite uniform from near the top of the unit to a depth of about 1080 m (Figure 17). No substantive change in inclination occurs across any of the thin bedded intervals which occur at depths of 860, 911, 934.1, and 952.4 m [Scott and Castellanos, 1984] indicating that the entire unit was emplaced rapidly with respect to secular variation. Below this depth the inclination record becomes increasingly irregular. This zone is also characterized by increasing alteration (to zeolites and clay) of the tuff with depth [Scott and Castellanos, 1984], suggesting that the greater variations in the inclination record is a result of the acquisition of secondary components of remanence during the alteration of the tuffs. The inclination record from USW G-1 is relatively uniform in the upper 20 m, rather irregular for the next 50 m, again relatively uniform for 100 to 125 m, and then increasingly erratic in the lowermost 90 m of the unit (Figure 17). No reason is readily apparent for the irregular record between the depths of 825 and 875 m. However, as in USW G-3, the irregular record from the lower portion of the Tram Member corresponds to a zone of increased alteration [Spengler and others, 1981]. The Tram Member encountered in USW G-2 is relatively thin, lithic-rich and argillized [Maldonado and Koether, 1983]. It yields an extremely erratic inclination record throughout its thickness.

The upper lithic-poor portion of the Tram Member is characterized by high remanent intensities (Table 15) which increase from values of a few tenths to one  $\text{Am}^{-1}$  near the top of the unit to maxima in the interior of the unit of nearly 6 and 15  $\text{Am}^{-1}$  at USW G-1 and G-3, respectively (Figure 18). As the magnetization decreases below these maxima the degree of welding also tends to decrease while the lithic content and the degree of alteration increase [Spengler and others, 1981; Scott and Castellanos, 1984]. Within this upper zone, changes in susceptibility correlate highly with changes in remanent intensity.

The lithic-rich lower zone is characterized by much lower remanent intensities than the upper zone (Table 15). Maldonado and Koether [1983] divide this portion of the Tram Member in drill hole USW G-2 into two parts, a unit consisting of more than 50% lithics above a depth of 1135 m and one comprising less than 50% lithics below this depth. As can be seen in Figure 18 both susceptibility and remanent intensity curves change abruptly at this depth. Although magnetization remains low throughout the lower lithic-rich altered portion of the Tram Member in USW G-1 and G-3, susceptibilities between 995-1060 m in USW G-1 and in the lowermost 75 m of the unit in USW G-3 are of about the same magnitude as those in the lithic-poor upper portion.

Table 14. Directional data for the Tram Member

Site	Lat.	Long.	N	$D_R$	$I_R$	$a_{95}$	K	af	Comments
USMG-1	36.867	116.458	6	135.8	-50.6	1.6	1762.8	10	Depth 935.5-938.5 m.
USW G-3	36.818	116.467	26	138.7	-42.6	3.2	81.1	10	Depth 819.5-940.5 m.

For explanation of headings see Table 1.

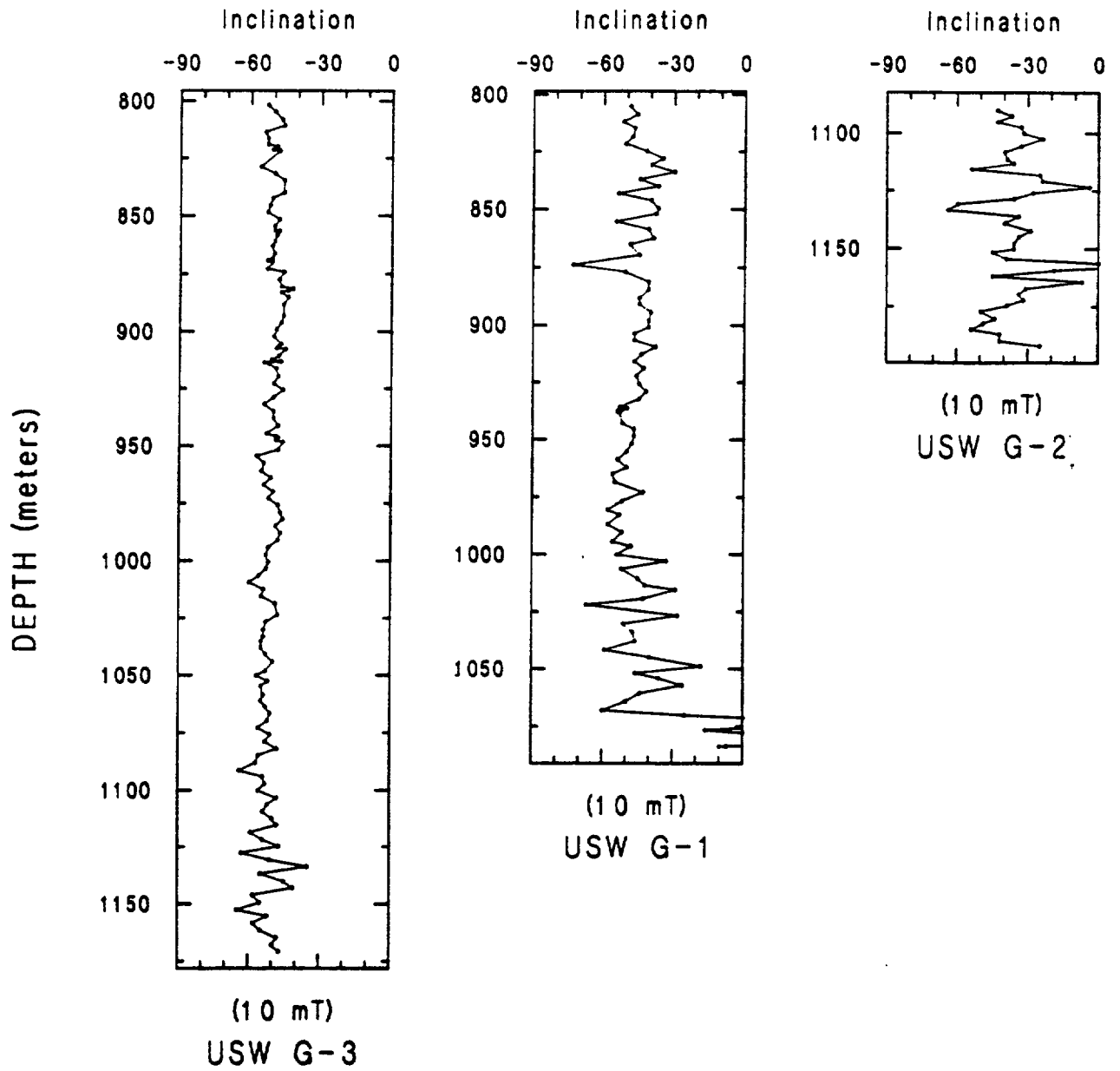


Figure 17.—Paleomagnetic inclinations versus depth for the Tram Member of the Crater Flat Tuff after a demagnetization at a peak field of 10 mT.

Table 15. Magnetic Property data for the Tram Member

Site	N	$J_{NRM}$	Sus.	Q	$D_T$	$I_T$	$J_T$	Comments
USW G-1	86	1.29±1.37	3.46±2.19	7.69	131	-30	1.20±1.30	Assumed $D_R=144^\circ$ .
	48	2.20±1.20	4.80±1.27	10.7	141	-42	2.04±1.17	Depth 805.0-945.5 m. Upper Tram
	38	.137±.143	1.73±1.87	3.89	117	-4	.125±.115	Depth 948.0-1073.5 m. Lower Tram
USW G-2	41	.217±.601	1.43±2.17	2.71	124	-1	.187±.546	Assumed $D_R=144^\circ$ .
USW G-3	139	1.90±2.40	2.90±1.65	13.3	134	-41	1.81±2.36	Assumed $D_R=145^\circ$ .

For explanation of headings see Table 2.

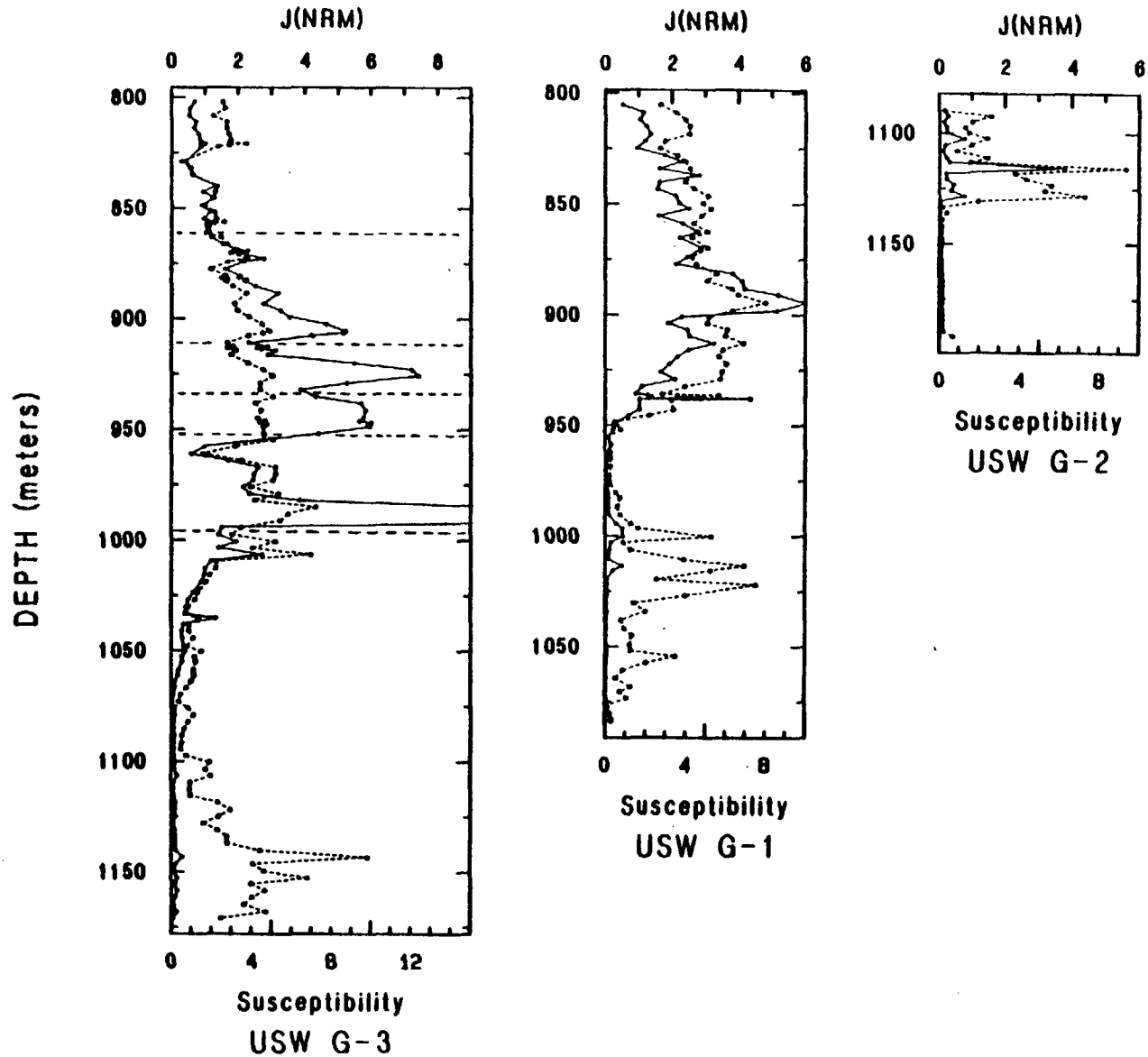


Figure 18.—Intensity of natural remanent magnetization,  $J(\text{NRM})$ , in  $\text{Am}^{-1}$  (circles and solid line) and SI susceptibility  $\times 10^3$  (squares and dashed line) for the Tram Member of the Crater Flat Tuff. Horizontal dashed lines in plot of USW G-3 data represent depositional breaks [Scott and Castellanos, 1984].

Comparison of the magnetic properties to the lithologic description of the Tram Member from drill hole USW G-3 [Scott and Castellanos, 1984] reveals a good correspondence between geologically recognizable breaks in deposition and changes in magnetic properties. Scott and Castellanos [1984] recognized at least five depositional breaks. The upper four occur at depths of about 860, 911, 934 and 952.4 m and are marked by the presence of thin bedded tuffs. The fifth occurs at about 994 m at the base of an ash flow and was recognized by a minimum in the degree of welding. One of the four largest remanent intensity maxima occurs between each pair of adjacent depositional breaks (Figure 18) and the breaks fall at or near intensity and susceptibility minima. The largest of these maxima occurs just below a vitrophyre (982.1-983.7 m) [Scott and Castellanos, 1984]. A similar relationship between magnetic properties and a depositional break was noted for the Bullfrog Member. These observations and those of Hatherton [1954a; 1954b] indicate that at least some of the variation in magnetization may be related to the depositional history of the tuff. The mechanisms responsible for these variations are unknown but may include: (1) variation of the composition (i.e. magnetite content) of the erupted magma with time; (2) post-emplacment growth of fine-grained magnetic phases which occurs to a greater extent in one portion of the flow than another (perhaps more time for growth in the more slowly cooling interior than at the flow margins); and (3) greater oxidation of fine-grained magnetite at the top and bottom of the flows either at high temperature (during cooling) or at low temperature. Regardless of the mechanism, the correlation between remanent intensity variations and depositional breaks suggests that these variations could provide a useful tool for mapping the internal stratigraphy of thick compound cooling units.

#### Other Units

##### Lava Flows and Flow Breccias between Tram Member and Tuff of Lithic Ridge:

The dacite and rhyodacite lava flows and flow breccias underlying the Tram Member in the northern part of Yucca Mountain [Spengler and others, 1981; Maldonado and Koether, 1983] were sampled throughout their vertical extent in drill holes USW G-1, G-2, and at four depth intervals in USW H-6. These units are not present in USW G-3.

The inclination data from USW G-1 and G-2 vary to such a degree that even a magnetic polarity (normal or reversed) for these rocks cannot be determined from these data (Figure 19). This erratic record may be due to alteration of the rocks, or it may indicate that the individual blocks comprising the breccia had cooled sufficiently to acquire their remanence prior to emplacement. In contrast, the dacite lava flows from USW H-6 yield exclusively downward directed magnetic vectors with inclinations ranging between 25° and 40° (Figure 19). Therefore, the unit is considered to be of normal polarity ( $D_R=0^\circ$ , was assigned for the calculation of the total magnetization, see Table 16).

In samples from USW G-1 and G-2 remanent intensity averages only a few tenths of an  $\text{Am}^{-1}$ ; however, susceptibility values are quite high (Figure 20 and Table 16). Intensities from two levels in USW H-6 are of similar magnitude to those in USW G-1 and G-2, and at two levels are much greater. Only samples of vitrophyre from a depth of 1100 m in USW H-6 have susceptibilities of the level observed in the other holes.

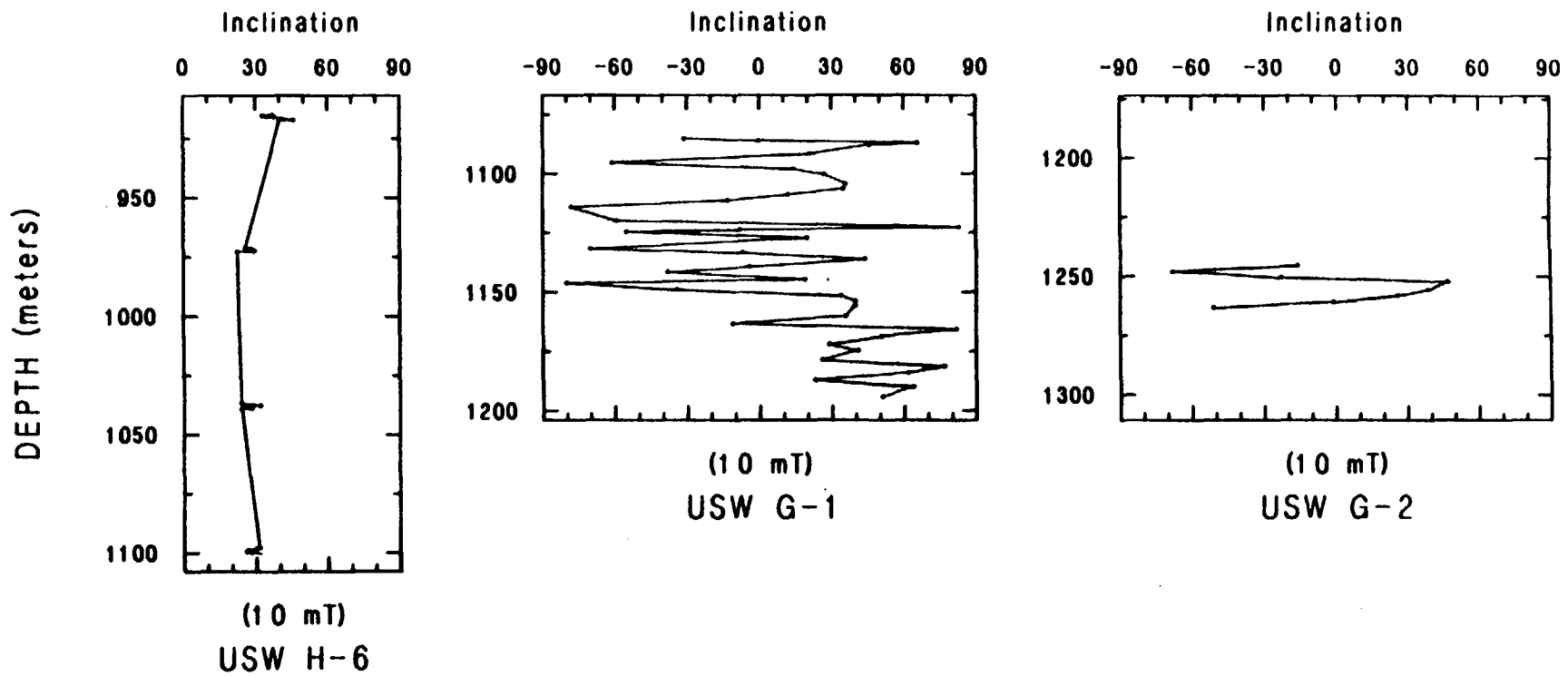


Figure 19.—Paleomagnetic inclinations versus depth for the dacite and rhyodacite lava flows and flow breccias between the Tram Member of the Crater Flat Tuff and the Lithic Ridge Tuff, after af demagnetization at a peak field of 10 mT.

Table 16. Magnetic Property data for the Dacite and Rhyodacite (between Tram and Lithic Ridge)

Site	N	$J_{NRM}$	Sus.	Q	$D_T$	$I_T$	$J_T$	Comments
USW G-1	41	.395±.243	14.45±7.29	0.71	8	49	.867±.450	Assumed $D_R=0^\circ$ .
USW G-2	8	.344±.142	29.50±5.05	0.27	10	51	1.13±0.25	Assumed $D_R=0^\circ$ .
USWH-6	24	1.29±1.31	7.44±6.91	4.16	3	40	1.56±1.52	Assumed $D_R=0^\circ$ .
	6	.117±.038	2.55±1.16	1.27	5	50	.216±.076	Depth 914.5-917.5 m.
	6	1.53±0.49	4.41±1.43	8.77	1	32	1.68±0.53	Depth 971.0-973.0 m.
	6	.404±.101	4.36±1.08	2.27	3	38	.558±.130	Depth 1036.5-1039.0 m.
	6	3.12±0.99	18.47±4.40	4.32	2	40	3.80±0.94	Depth 1097.5-1100.5 m.

For explanation of headings see Table 2.

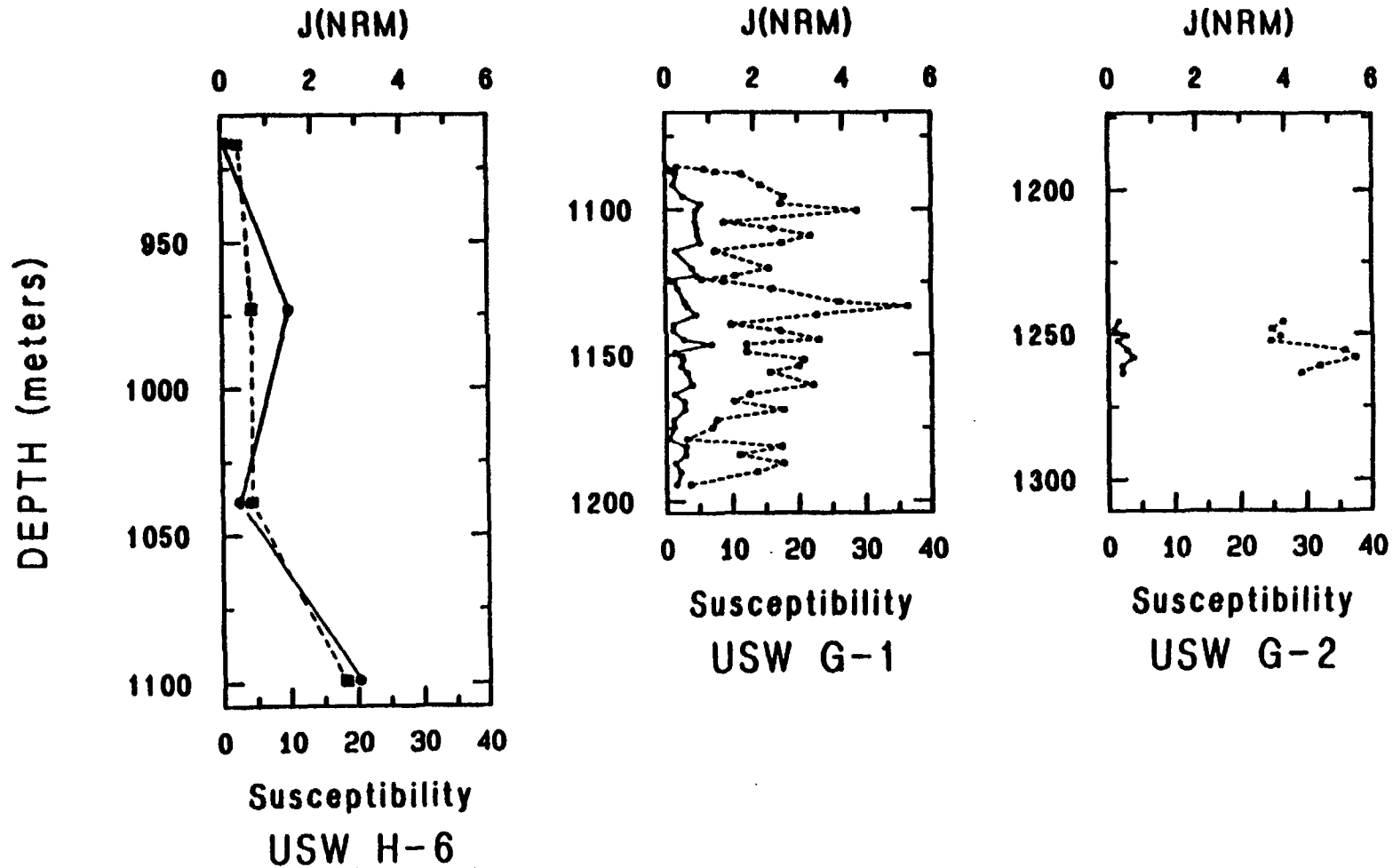


Figure 20.—Intensity of natural remanent magnetization,  $J(\text{NRM})$ , in  $\text{Am}^{-1}$  (circles and solid line) and SI susceptibility  $\times 10^3$  (squares and dashed line) for the dacite and rhyodacite lava flows and flow breccias between the Tram Member of the Crater Flat Tuff and the Lithic Ridge Tuff. Values plotted for USW H-6 are each averages of six values (see Table 16).

The rock obtained from USW H-6 appears to be much less altered than that from USW G-1 and G-2. In addition, values of Q computed for the various levels sampled in USW H-6 are substantially greater than those obtained from USW G-1 and G-2. These observations suggest that alteration has destroyed much of the fine-grained magnetite at the USW G-1 and G-2 localities, and that if these rocks were unaltered they would possess much higher remanent intensities.

**Lithic Ridge Tuff:** The Lithic Ridge Tuff was sampled throughout its thickness in drill holes USW G-1, G-2, and G-3. Oriented specimens were obtained from all three of these holes as well as from outcrop at the type locality at Lithic Ridge (site JR81-10) [Carr and others, 1984]. Although the inclination data from the entire unit as a whole are extremely erratic (Figure 21), af demagnetization of the oriented specimens yielded mean directions of remanent magnetization from each of the three drill holes that are to the southwest and nearly horizontal (Table 17). The mean directions of remanent magnetism of the outcrop samples after af demagnetization at 5, 10 and 20 mT differ significantly from those obtained from the drill holes (Figure 22 and Table 17). However, the average direction of vectors removed during demagnetization between 5 and 20 mT is in good agreement with the directions determined from the three holes (Figure 22f). The outcrop samples apparently possess both a soft remanence (probably a viscous remanence), which is largely removed by af demagnetization in a peak field of 5 mT (Figure 22b), and a rather hard, secondary magnetization (probably a chemical remanent magnetization) which remains after demagnetization at 20 mT (Figure 22a). These components tend to obscure the initial remanence of the unit. Similar components may be present in the drill hole samples and account for the irregular inclination records.

It should be noted that the directions presented in Table 17 and Figure 22 have not been corrected for tectonic rotation. This implies that the Lithic Ridge Tuff at Yucca Mountain has a similar attitude to that at the type locality. Nevertheless, the good agreement of directions from this unit at Yucca Mountain and at the type locality strongly supports the equivalence of these rocks.

Variations in remanent intensity of the Lithic Ridge Tuff with depth display a high degree of correlation with susceptibility variations (Figure 23). Average intensities from the drill holes are less than  $0.2 \text{ Am}^{-1}$  and from outcrop only slightly higher (Table 18). Both susceptibility and intensity generally decrease with depth. This may be due to increasing alteration with depth, although such a change is not evident from petrographic descriptions of the core [Spengler and others, 1981; Maldonado and Koether, 1983; and Scott and Castellanos, 1984].

**Older Tuffs of USW G-1, and Lava Flows and Flow Breccias of USW G-2;** Spengler and others [1981] divide the older tuffs encountered in drill hole USW G-1 into three units, A, B, and C. Inclination data from these tuffs are for the most part erratic. Because of the highly altered nature of these rocks it is impossible to confidently interpret magnetic polarities for these ash-flow tuffs. Nevertheless, two zones from which oriented samples were obtained yield reasonably consistent directions. One, from unit C at the bottom of drill hole USW G-1, is normal; the other, from rocks at the bottom of USW G-3 which correlate with unit A [Scott and Castellanos, 1984], is reversed (Table 19).

Table 17. Directional data for the Lithic Ridge Tuff

Site	Lat.	Long.	N	D <sub>R</sub>	I <sub>R</sub>	a <sub>95</sub>	K	af	Comments
JR81-10	36.933	116.269	16	260.6	41.9	14.2	7.7	20	Type locality [Carr and others, 1984]. *
			16	305.0	64.6	18.4	5.0	HRM-5	Removed vector.
			13	243.5	5.4	5.6	55.4	5-10	" "
			13	239.6	-0.3	6.7	30.8	5-20	" "
			13	238.4	-3.1	7.6	30.8	10-20	" "
USW G-1	36.867	116.458	8	225.3	-7.0	5.1	118.2	30	Depth 1229.0-1205.0 m.
USW G-2	36.890	116.459	10	229.4	-8.5	11.4	18.9	10	Depth 1313.0-1322.0 m.
USW G-3	36.818	116.467	9	236.2	-7.1	10.1	26.8	10	Depth 1183.5-1310.0 m.

For explanation of headings see Table 1.

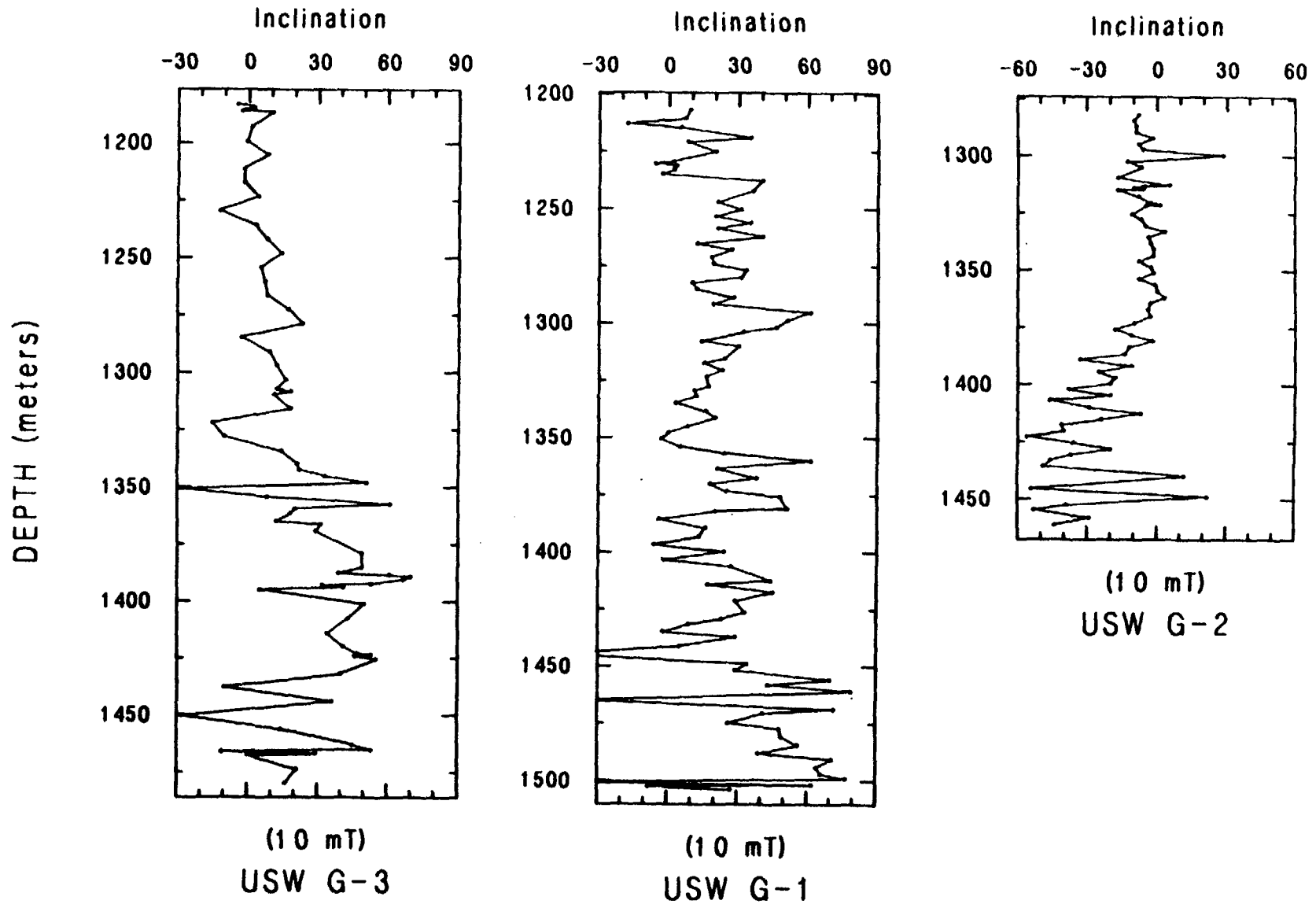


Figure 21.—Paleomagnetic inclinations versus depth for the Lithic Ridge Tuff after af demagnetization at a peak field of 10 mT.

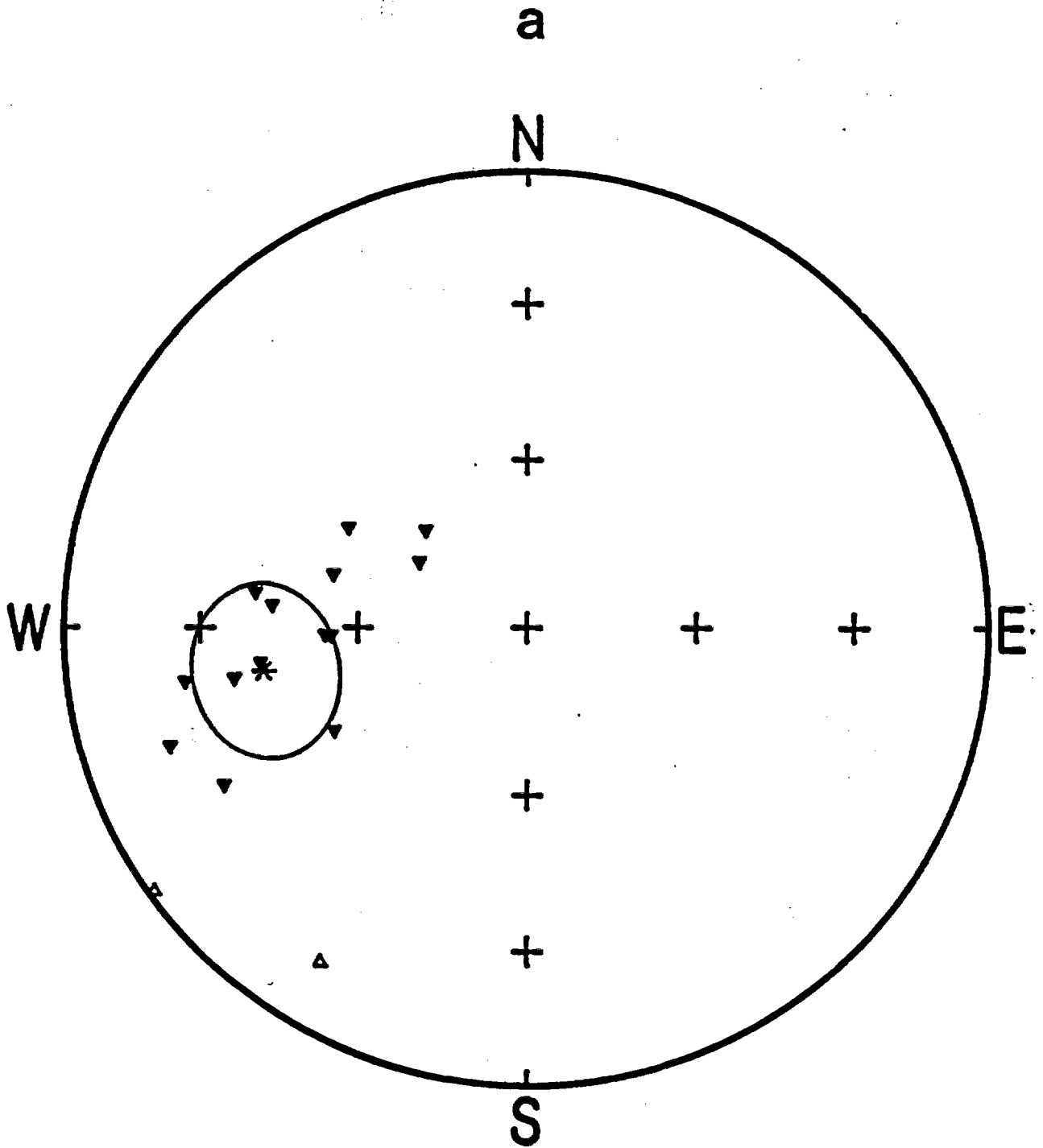


Figure 22.—Equal area projections of paleomagnetic directions from the Lithic Ridge Tuff: a through e are results from site JR81-10 at Lithic Ridge [Carr and others, 1984] (see Table 17); \* is mean direction, solid triangles are sample directions on lower hemisphere, open triangles are sample directions on upper hemisphere, circles are sample directions not included in calculation of the mean (all are on lower hemisphere) a) residual vectors after af demagnetization at 20 mT; b) vectors removed between NRM and 5 mT; c) vectors removed between 5 and 10 mT; d) vectors removed between 10 and 20 mT; e) vectors removed between 5 and 20 mT; f) mean directions of remanent magnetization and associated cone of 95% confidence from drill holes USW G-1, G-2, G-3 after af demagnetization at peak fields of 30, 10, and 10 mT, respectively, and of vectors removed between 5 and 20 mT for site JR81-10.

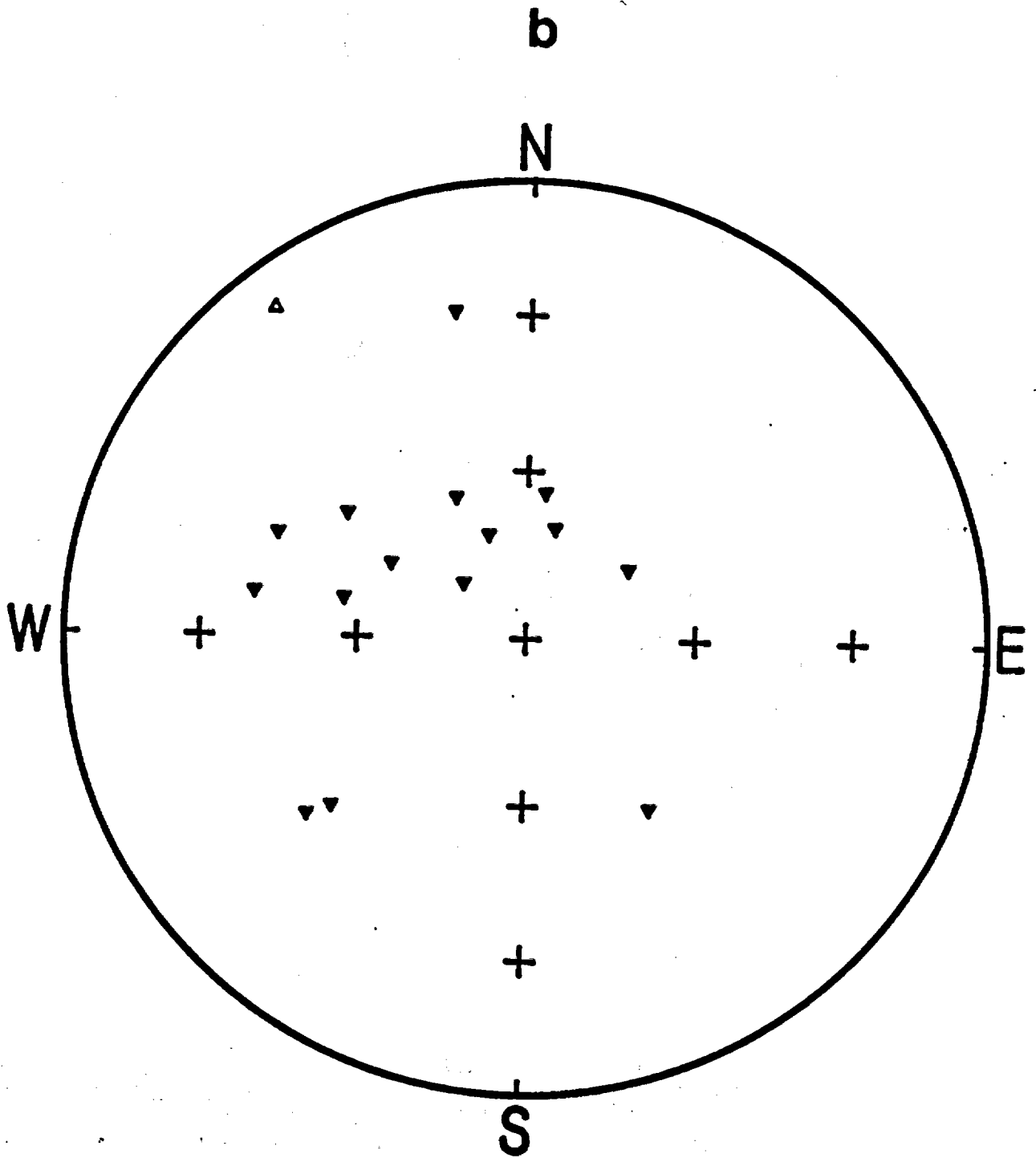


Figure 22.—continued

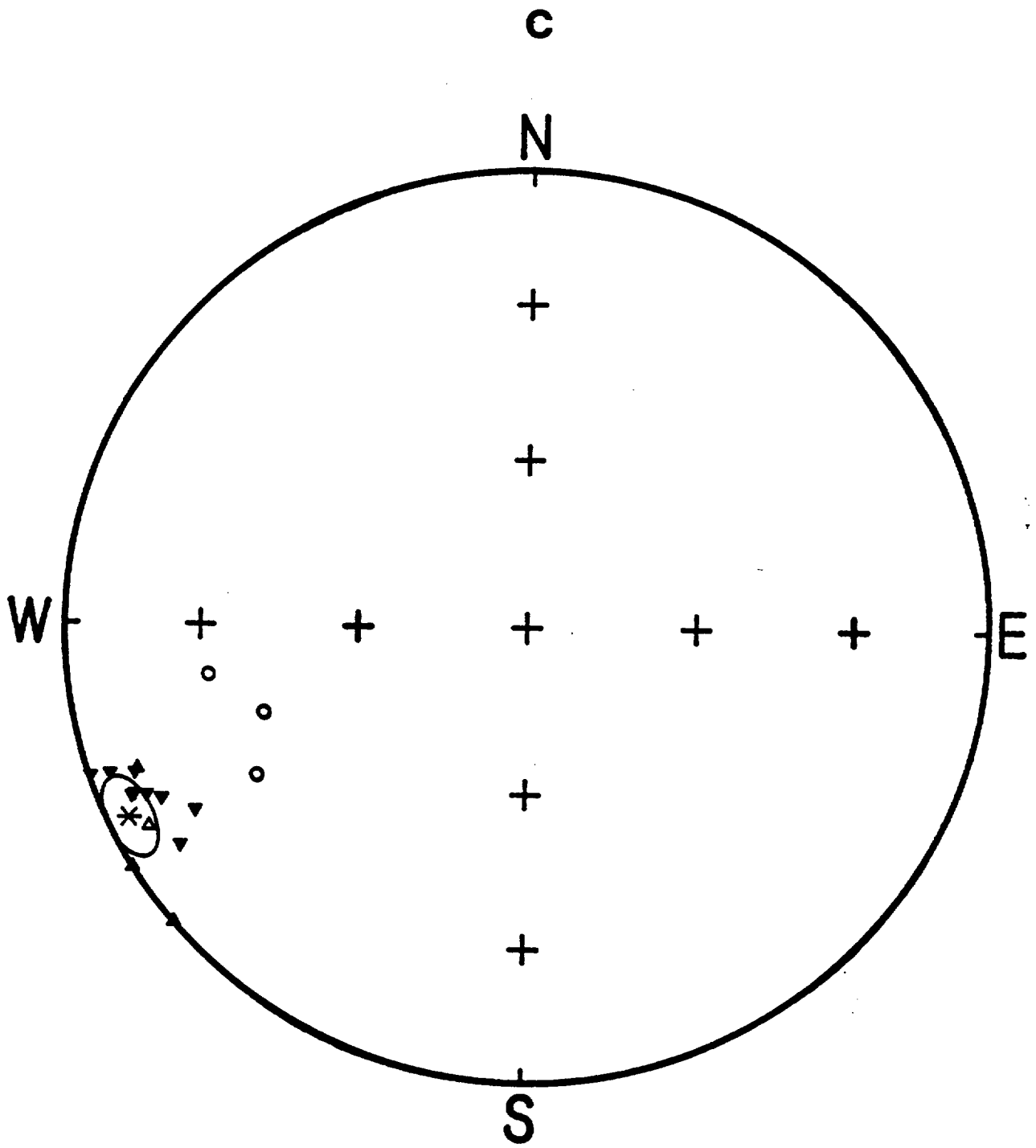


Figure 22.—continued

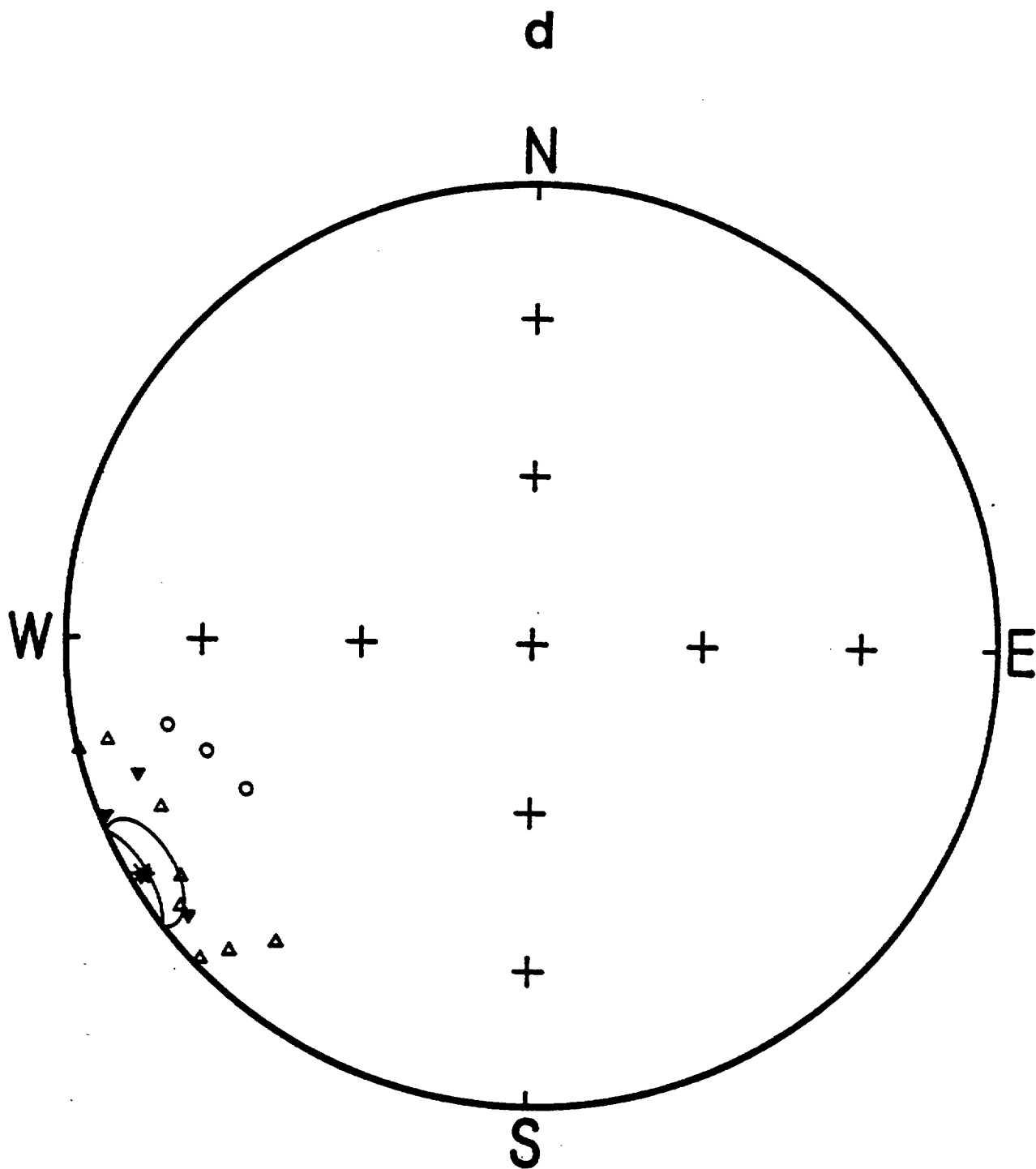


Figure 22.—continued

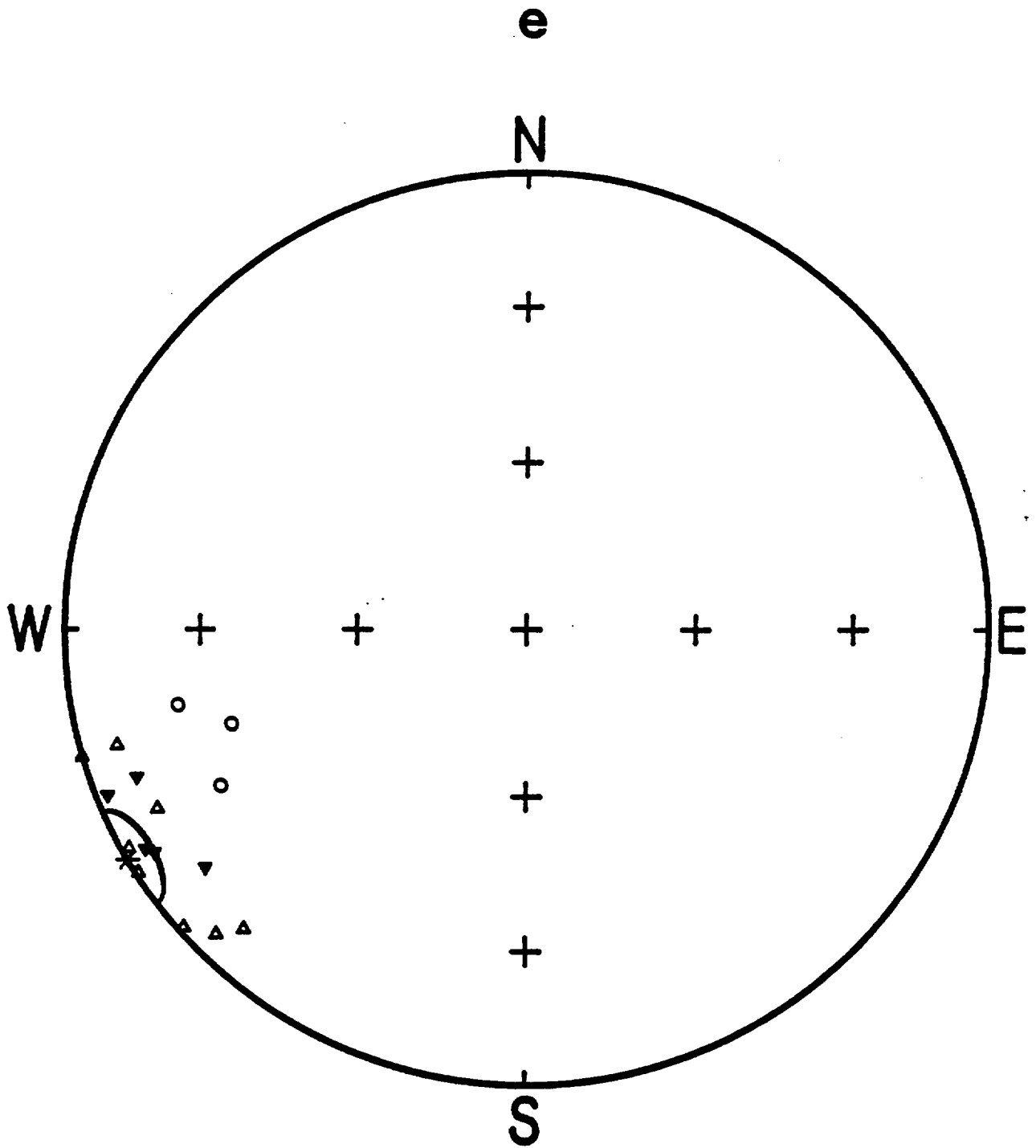


Figure 22.-continued

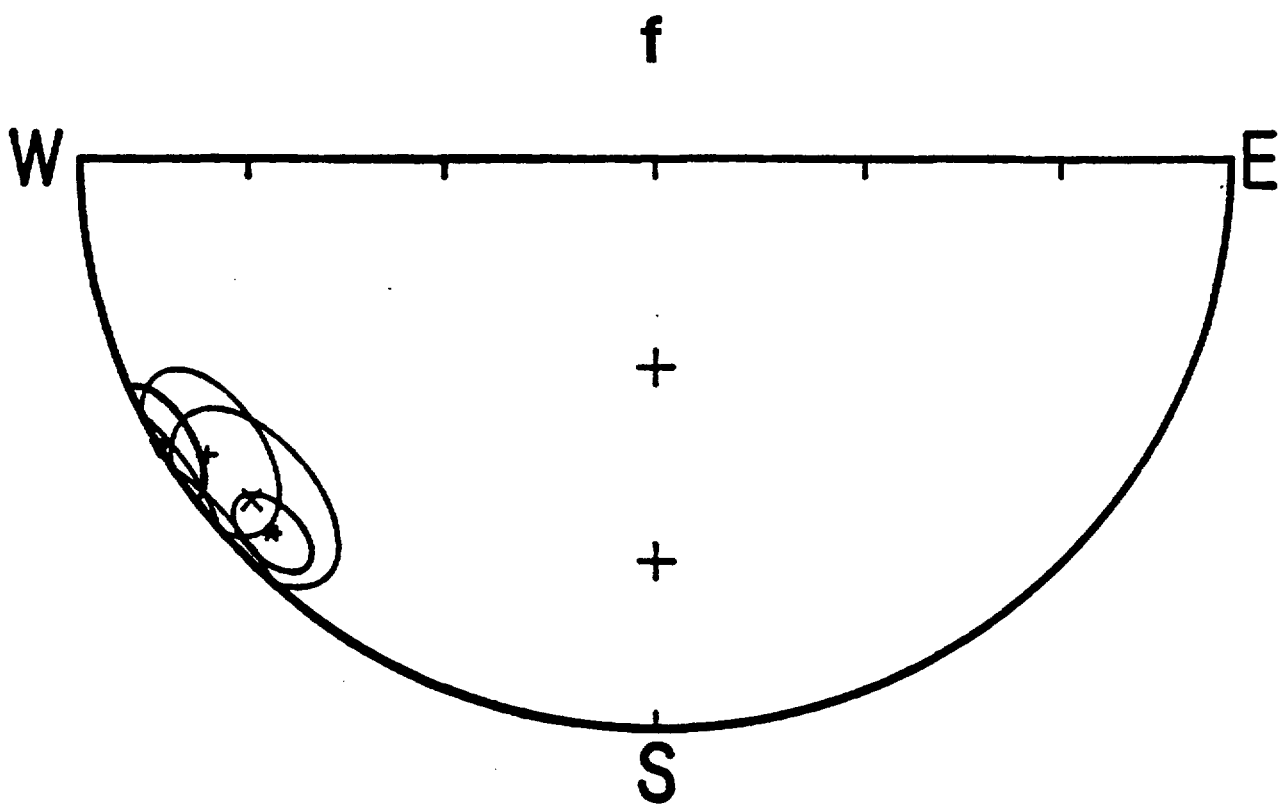


Figure 22.—continued

Table 18. Magnetic Property data for the Lithic Ridge Tuff

Site	N	$J_{NRM}$	Sus.	Q	$D_T$	$I_T$	$J_T$	Comments
JR81-10	16	.265±.072	4.59±0.73	1.41	260	42	.290±.087	
USW G-1	95	.171±.165	3.14±2.20	1.19	251	69	.222±.182	Assumed $D_R=225^\circ$ .
USW G-2	73	.134±.134	2.58±1.91	1.23	249	48	.132±.121	Assumed $D_R=225^\circ$ .
USW G-3	75	.175±.142	3.72±2.71	1.19	264	62	.226±.138	Assumed $D_R=235^\circ$ .

For explanation of headings see Table 2.

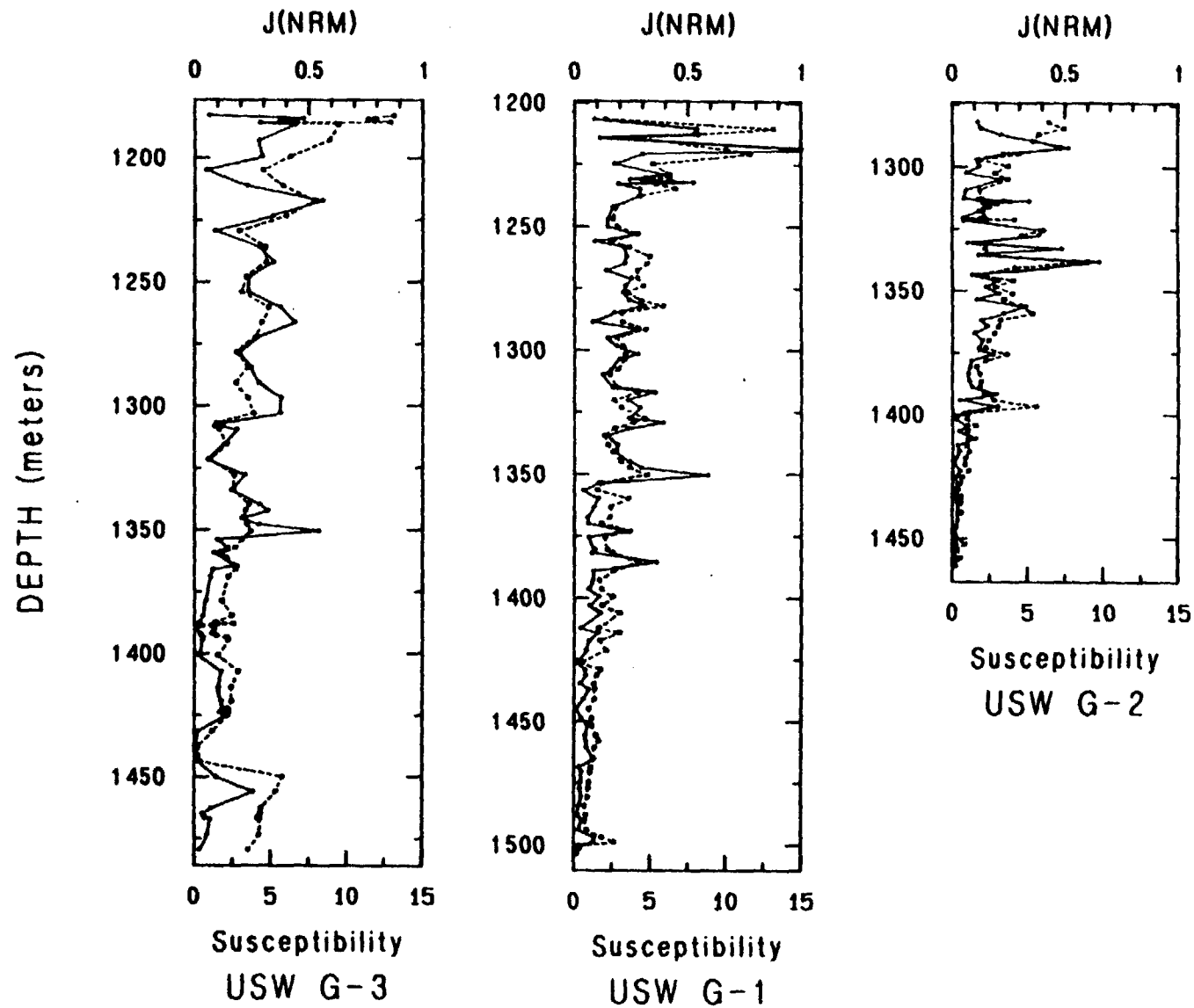


Figure 23.—Intensity of natural remanent magnetization,  $J(NRM)$ , in  $A m^{-1}$  (circles and solid line) and SI susceptibility  $\times 10^3$  (squares and dashed line) for the Lithic Ridge Tuff.

The thick sequence of older ash flows penetrated in the bottom of USW G-1 is not present in USW G-2. Only a single thin ash-flow tuff which apparently correlates with a thin tuff at the top of unit C represents this part of the section [Maldonado and Koether, 1983]. A sequence of lava flows and flow breccias occurs below this tuff at the locality of USW G-2. With increasing depth the composition of these flows changes from rhyolite, to quartz latite, and finally to dacite. These rocks are highly altered. All but two of 33 samples of the rhyolite have negative remanent inclinations, whereas all 40 samples of the quartz latite and 21 samples of the dacite have positive inclinations. Therefore, the rhyolite appears to be of reversed polarity while the older more mafic lavas are of normal polarity.

The average magnetic properties for units penetrated in drill holes USW G-1, G-2 and G-3 below the Lithic Ridge Tuff are summarized in Table 20. Total magnetizations for these rocks are plotted in Figure 24.

The uppermost part of unit A in USW G-1 and all of the unit sampled from USW G-3 are characterized by extremely low remanent intensities ( $\ll 0.1 \text{ Am}^{-1}$ ) and susceptibilities ( $< 2 \times 10^{-3} \text{ SI}$ ). Both intensity and susceptibility values then rise so that  $J_t$  averages about  $0.45 \text{ Am}^{-1}$  in the lower part of unit A in USW G-1 (Figure 24). Total magnetization of unit B averages about  $0.3 \text{ Am}^{-1}$  near the top of the unit, falls to extremely low values near the middle, and then rises sharply near the base of the unit. Unit C from USW G-1 is on average more magnetic than units A and B, although its total magnetization curve varies erratically.

The composition of the lavas and flow breccias which occur beneath the Lithic Ridge Tuff in USW G-2 (and presumably stratigraphically below Unit C of USW G-1) progress from rhyolite, to quartz latite, to dacite with depth [Maldonado and Koether, 1983]. Although these rocks are highly altered, they become more magnetic with depth and as their compositions become more mafic.

#### DISCUSSION AND SUMMARY

The interpretation of these data bear on stratigraphy, structure, and potential sources of magnetic anomalies in the vicinity of the Nevada Test Site. The data also raise several questions about the magnetism of welded tuffs.

Based upon the paleomagnetic directional data, declinations and inclinations from oriented specimens and inclination data from unoriented samples, the units can be assigned the polarities given in Table 21. Due to various uncertainties, such as the directional variations demonstrated in the Topopah Spring Member of the Paintbrush Tuff and orientation errors of unknown magnitude in obtaining oriented cores from drill holes, and due to the fact that nearly all the data come from the Yucca Mountain block, no attempt has been made to define a precise direction of remanence for any of the units.

The polarity of the units is useful as a stratigraphic aid. For instance the petrographically similar Topopah Spring and Tiva Canyon Members of the Paintbrush Tuff are easily distinguished by their opposite polarities. In addition, the Lithic Ridge Tuff possesses very unusual (southwesterly and nearly horizontal) remanent direction. Because the geomagnetic field would not be expected to maintain a direction such as this for extended periods or

**Table 19. Directional data for the Older Tuffs of USW G-1**

Site	Lat.	Long.	N	D <sub>R</sub>	I <sub>R</sub>	a <sub>95</sub>	K	af	Comments
USW G-1	36.867	116.458	5	339.0	52.3	4.8	258.6	20	Depth 1822.5-1829.0 m. Unit C.
USW G-3	36.818	116.467	6	161.9	-59.7	5.3	158.2	10	Depth 1429.0-1533.5 m. Unit A.

For explanation of headings see Table 1.

Table 20. Magnetic Property data for Rocks Older than the Lithic Ridge Tuff

Site	N	J <sub>NRM</sub>	Sus.	Q	D <sub>T</sub>	I <sub>T</sub>	J <sub>T</sub>	Comments
USW G-1	38	.142±.130	3.93±2.94	0.79	61	75	.277±.231	Unit A. Assumed D <sub>R</sub> =150°. Depth 1506-1620 m.
	14	.097±.066	5.96±4.89	0.72	41	66	.328±.230	Unit B. Assumed D <sub>R</sub> =100°. Depth 1623-1656 m.
	76	.288±.263	11.0±11.4	0.89	17	53	.700±.537	Unit C. Assumed D <sub>R</sub> =20°. Depth 1658-1829 m.
USW G-2	33	.202±.456	1.66±1.91	9.43	173	-1	.200±.433	Rhyolite. Assumed D <sub>R</sub> =180°. Depth 4877-5202 m.
	40	.417±.419	3.52±6.20	26.6	3	57	.560±.578	Quartz latite. Assumed D <sub>R</sub> =0. Depth 5211-5628 m.
	21	1.30±0.92	43.4±11.6	0.74	9	60	3.06±1.22	Dacite. Assumed D <sub>R</sub> =0. Depth 5680-5885 m.
USW G-3	14	.015±.006	1.13±1.39	0.60	316	81	.0.36±.060	Unit A. Assumed D <sub>R</sub> =200°. Depth 1485-1533 m.

For explanation of headings see Table 2.

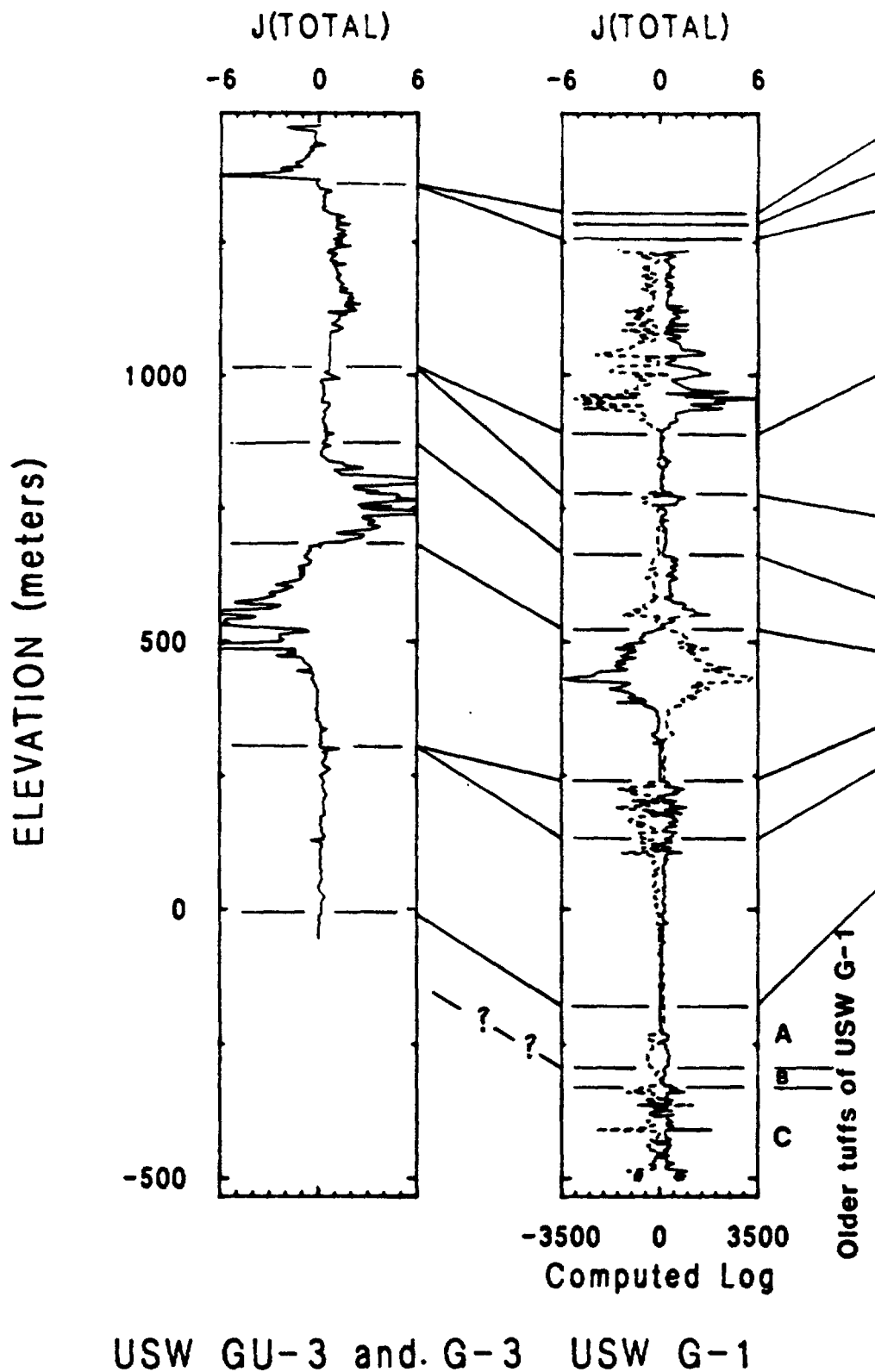
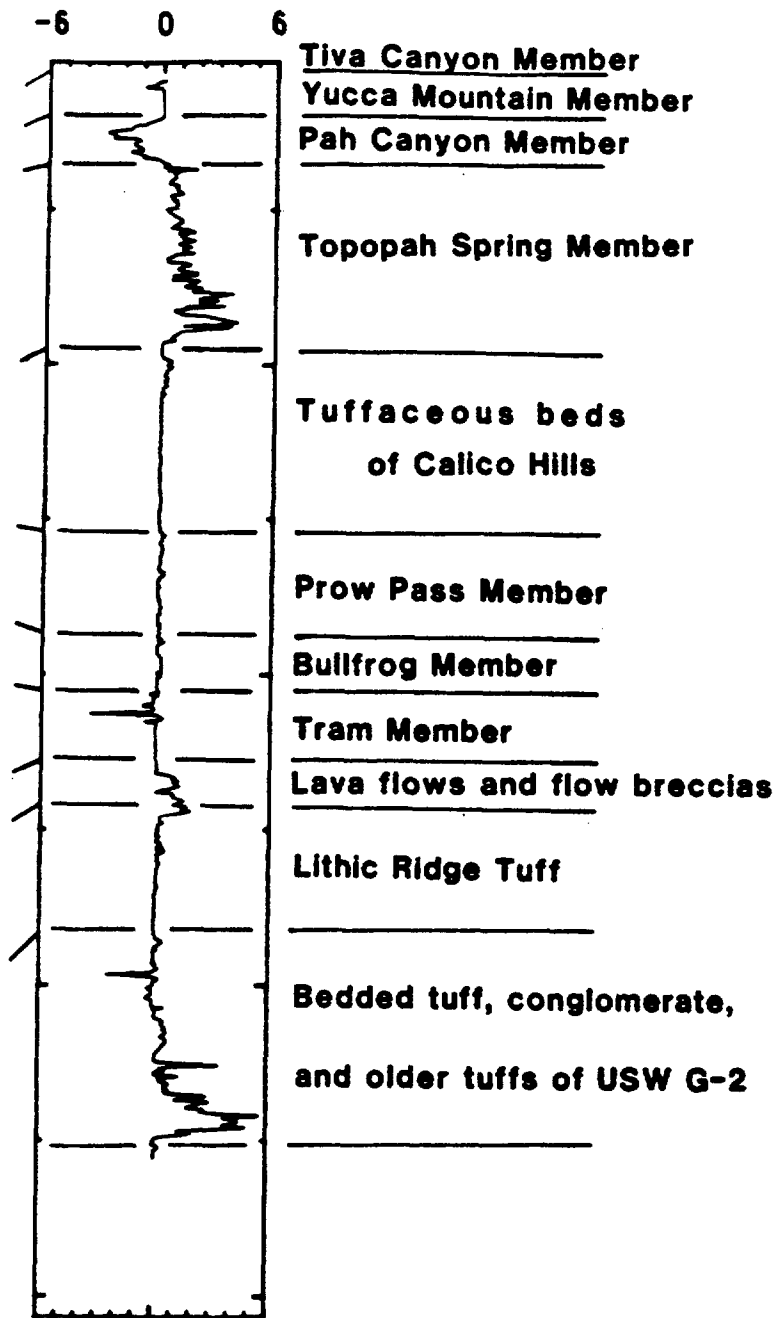


Figure 24.—Total magnetization ( $\text{Am}^{-1}$ ) versus depth (solid lines) for drill holes USW G-1, G-2, GU-3, and G-3, and modeled total field log (dashed

J(TOTAL)



USW G-2

line) for drill hole USW G-1 (nT). Geologic contacts are from Spengler and others [1981], Maldonado and Koether [1983], and Scott and Castellanos [1984].

Table 21. Paleomagnetic Polarities of Volcanic Rocks at Yucca Mountain

Unit	Polarity	Comments
<b>Paintbrush Tuff:</b>		
Tiva Canyon Member	R	Consistent directions.
Yucca Mountain Member	R	Inclination about 40°.
Pah Canyon Member	R	Inclination greater than 60°.
Topopah Spring Member	N	Variable directions.
Tuffaceous beds of Calico Hills	N	
<b>Crater Flat Tuff:</b>		
Prow Pass Member	N	
Bullfrog Member	N	
Tram Member	R	
Dacite and Rhyodacite (in USW G-1, G-2, and H-6)	N?	Based on inc. data from USW H-6.
Lithic Ridge Tuff	Intermediate	Nearly horizontal to the southwest.
<b>Older Tuffs of USW G-1:</b>		
A	R?	Based on oriented core from USW G-3.
B	?	
C	N?	Based on oriented core from USW G-1.
<b>Lavas in USW G-2:</b>		
rhyolite	R	Based on inclination data.
quartz latite	N	Based on inclination data.
dacite	N	Based on inclination data.
Older tuffs of USW G-2	?	

to frequently occupy such a position, determination of this direction from other localities would strongly support correlation to the Lithic Ridge Tuff.

In addition, inclination data from the tuffaceous beds of Calico Hills suggest that the relatively thin section encountered in drill hole USW G-1 is correlative with only the lowermost 125 m or so of the much thicker section encountered in drill hole USW G-2.

Two points bearing upon the structure of Yucca Mountain should be emphasized. First, paleomagnetic directions from the Tiva Canyon Member of the Paintbrush Tuff indicate that there has been no relative rotation of more than a few degrees between the sampling sites after emplacement of this unit. Therefore, the rather large, sharp change in strike observed in both the eutaxitic foliation and the base of the Tiva Canyon Member is not due to rotation about a vertical axis, and may be either a depositional feature or due to small rotations about horizontal axes. Second, the acquisition of data demonstrating very large directional variations of the remanent magnetism of the Topopah Spring Member largely invalidate the paleomagnetic evidence for left-lateral strike-slip movement on faults within Drill Hole Wash [Spengler and Rosenbaum, 1980].

Bath and others [1983] have arbitrarily set the following limits to characterize rocks for the purpose of describing their potential for producing magnetic anomalies:

nonmagnetic < 0.05 Am<sup>-1</sup>  
0.05 Am<sup>-1</sup> < weakly magnetic < 0.50 Am<sup>-1</sup>  
0.50 Am<sup>-1</sup> < moderately magnetic < 1.50 Am<sup>-1</sup>  
1.50 Am<sup>-1</sup> < strongly magnetic.

Inspection of Figure 24 reveals that there are four areally extensive ash-flow sheets which possess moderate to strong magnetizations throughout substantial stratigraphic thicknesses, and are therefore considered to be likely sources of magnetic anomalies. These units are the Tiva Canyon and Topopah Spring Members of the Paintbrush Tuff, and the Bullfrog and Tram Members of the Crater Flat Tuff. The Tiva Canyon and Tram Members are reversed, and the other two units are of normal polarity. Although data from only three samples of the tuff of Chocolate Mountain (the intracaldera equivalent of the uppermost layers of the Tiva Canyon Member) are available, this unit appears to be highly magnetic and certainly must be considered as a possible anomaly source. The reversely magnetized Pah Canyon Member is also moderately to strongly magnetic. However, it is not considered to be an important source of magnetic anomalies because it is thin and of limited areal extent. Also, the lavas between the Tram Member of the Crater Flat Tuff and the Lithic Ridge Tuff reach moderate to strong magnetizations (Figures 20 and 24, and Table 18). The thickness of this unit varies greatly (Figure 20), and it therefore must be considered a possible anomaly source.

In addition to the units penetrated in drill holes at Yucca Mountain there obviously may be deeper anomaly sources. Possible deep sources include other volcanic rocks, plutonic rocks, and altered sediments like those encountered in drill hole UE25a-3 at Calico Hills [Baldwin and Jahren, 1982].

The results raise two major questions about the magnetization of welded tuffs. The cause of variations in the directional data from the Topopah

Spring Member are presently unknown. Several possible explanations are: 1) that the entire unit was emplaced over a relatively long period of time with respect to secular variation; 2) that the unit was emplaced quickly but cooled over a relatively long period; and 3) that internal deformation of the cooling unit took place at temperatures below that at which much of the magnetization was acquired. Regardless of the cause, such variations severely limit the usefulness of paleomagnetic directions from the Topopah Spring Member as an aid to structural interpretation.

The other question concerns the origin of the large lateral and vertical variations of magnetic properties observed within single cooling units. Mechanisms which could contribute to the variations include: (1) differences within the magma in composition, quantity, and grain size of the magnetic phase at the time of eruption; (2) post-emplacment growth of differing quantities and grain sizes of magnetic phases; and (3) varying degrees of alteration with attendant oxidation of highly magnetic magnetite to less magnetic hematite. The position of remanent intensity maxima between depositional breaks in the Bullfrog and Tram Members of the Crater Flat Tuff encountered in drill hole USW GU-3 and G-3 (Figures 16 and 18) strongly suggests some relation of the magnetic property variations to emplacement history.

Figure 24 displays a calculated magnetic field log for drill hole USW G-1. The model used to generate the log consists of a large number of thin sheets. Each sheet corresponds to a sample and extends half the distance to the overlying sample and half way to the underlying one. Each sheet was assigned a uniform magnetization equal to the total magnetization computed for the corresponding sample. The magnetic field produced by the model was calculated at about 3 m (10 ft) depth intervals at the center of a hexagonal hole approximately 0.3 m (1 ft) in diameter. The modeling results indicate that the magnetic field variations should have amplitudes of several hundred to several thousand nT. There is therefore a good possibility of using magnetization variations, as determined from in-hole magnetic logs in closely spaced holes, as an aid in locating not only major stratigraphic contacts but also to map zones within complex compound cooling units.

#### REFERENCES CITED

- Baldwin, M. J., and Jahren, C. E., 1982, Magnetic properties of drill core and surface samples from the Calico Hills area, Nye County, Nevada, U. S. Geological Survey, Open-File Report 82-536, 27 p.
- Bath, G. D., and Jahren, C. E., 1984, Interpretations of magnetic anomalies at a potential repository site located in the Yucca Mountain area, Nevada Test Site, U. S. Geological Survey, Open-File Report 84-120, 53 p.
- Bath, G. D., Jahren, C. E., Rosenbaum, J. G., and Baldwin, M. J., 1983, Magnetic investigations, Chapter C in Geologic and Geophysical investigations of Climax Stock intrusive, Nevada, U. S. Geological Survey, Open-File Report 83-377, p. 40-77.

- Byers, F. M., Carr, W. J., Orkild, P. P., Quinlivan, W. D., and Sargent, K. A., 1976, Volcanic suites and related cauldrons of Timber Mountain-Oasis Valley caldera complex, southern Nevada, U. S. Geological Survey, Professional Paper 919, 70p.
- Carr, W. J., Byers, F. M., Jr., and Orkild, P. P., 1984, Stratigraphic and volcano-tectonic relations of Crater Flat Tuff and some older volcanic units, Nye County, Nevada, U. S. Geological Survey Open-File Report 84-114, 42p.
- Christiansen, R. L., Lipman, P. W., Carr, W. J., Byers, F. M., Jr., Orkild, P. P., and Sargent, K. A., 1976, The Timber Mountain-Oasis Valley caldera complex of southern Nevada, Geological Society of America Bulletin, v. 87, p 943-959.
- Christie, K. W., and Symons, D. T. A., 1969, Apparatus for measuring magnetic susceptibility and its anisotropy, Geological Society of Canada, Paper 69-41, 10 p.
- Creer, K. M., and Sanver, M., 1967, The use of the sun compass, in Methods in Paleomagnetism, Collinson, D. W., Creer, K. M., and Runcorn, S. K., ed., Elsevier Publishing Company.
- Hatherton, T., 1954a, The magnetic properties of the Whakamru ignimbrites, New Zealand Journal of Science and Technology, v. 35, p. 421-432.
- Hatherton, T., 1954b, The permanent magnetization of horizontal volcanic sheets, Journal of Geophysical Research, v. 59, p. 223-232.
- King, R. F., 1955, Remanent magnetism of artificially deposited sediments, Monthly Notices of the Royal Astronomical Society, Geophysical Supplement, v. 7, p. 115-134.
- Maldonado, F., and Koether, S. L., 1983, Stratigraphy, structure, and some petrographic features of Tertiary volcanic rocks at the USW G-2 drill hole, Yucca Mountain, Nye County, Nevada, U. S. Geological Survey Open-File Report 83-732, 83p.
- Rosenbaum, J. G., Larson, E. E., Hoblitt, R. P., and Fickett, F. R., 1979, A convenient standard for low-field susceptibility calibration, Review of Scientific Instruments, v. 50, p. 1027-1029.
- Scott, R.B., and Castellanos, M., 1984, Preliminary report on the geologic character of drill holes USW GU-3 and USW G-3, U. S. Geological Survey Open-File Report 84-491, 121p.
- Spengler, R. W., Byers, F. M., Jr., and Warner, J. B., 1981, Stratigraphy and structure of volcanic rocks in drill hole USW G-1, Yucca Mountain, Nye County, Nevada, U. S. Geological Survey Open-File Report 81-1349, 50p.
- Spengler, R. W., and Rosenbaum, J., G., 1980, Preliminary interpretations of geologic results obtained from boreholes, UE25a-4, -5, -6, and -7, Yucca Mountain, Nevada Test Site, U. S. Geological Survey, Open-File Report 80-929, 33p.